Chemistry and Structural Studies on the Dioxygen-Binding Copper–1,2-Dimethylimidazole System

Indrajit Sanyal,† Kenneth D. Karlin,*,† Richard W. Strange,‡ and Ninian J. Blackburn*,§

Contribution from the Department of Chemistry, The Johns Hopkins University, Baltimore, Maryland 21218, Daresbury Laboratory, Warrington Cheshire, WA4 4AD, U.K., and Department of Chemical and Biological Sciences, The Oregon Graduate Institute of Science & Technology, Portland, Oregon 97007

Received April 13, 1993•

Abstract: Studies of copper complexes with the 1,2-dimethylimidazole (Me_2im) system have provided insights into the factors which control dioxygen (O_2) binding and activation in imidazole (histidine) ligated copper complexes and proteins. A two-coordinate complex $[Cu(Me_2im)_2](PF_6)$ (**1**(PF_6)) is formed by the reaction of 1,2-dimethylimidazole with $[Cu(CH_3CN)_4](PF_6)$. Although **1** is unreactive toward O_2 or CO, reaction with one additional molar equivalent of Me_2im yields a three-coordinate complex $[Cu(Me_2im)_3](PF_6)$ (**2**(PF_6)) which reacts with O_2 ($Cu/O_2 = 2:1$, manometry), producing the EPR silent dioxygen adduct, formulated as $[Cu_2(Me_2im)_6(O_2)]^{2+}$ (**3**). The structure of **1** has been studied by X-ray crystallography; it crystallizes in the monoclinic space group $C2/c$ with $Z = 4$, $a = 14.877$ (2) Å, $b = 15.950$ (4) Å, $c = 6.931$ (4) Å, and $\beta = 108.54$ (2)°. The linear two-coordinate Cu(I) structure is typical and contains crystallographically equivalent Cu–N(imid) distances of 1.865 Å. The structures of **2** and **3** have been studied by X-ray absorption spectroscopy, using imidazole group-fitting and full curved-wave multiple scattering analysis. Complex **2** is best fit by a T-shaped structure involving two short (1.89 Å) and one longer (2.08 Å) Cu–N(imid) distances. Absorption edge data confirm that the dioxygen complex **3** should be formulated as a Cu(II)–peroxo species. The EXAFS of **3** can be fit by either of two models, **A** and **B**. Model **A** involves a four-coordinate species having a *trans*-μ-1,2-peroxo bridge, but the edge data do not fully support the presence of square planar coordination. Model **B**, which is more consistent with the edge data, involves a five-coordinate structure with a *bent* η^2-η^2-peroxo bridging between two coppers 2.84 Å apart. XAS studies on the crystallographically characterized complex $[\{Cu(TMPA)\}_2(O_2)]^{2+}$ (**4**) (TMPA = tris[(2-pyridyl)methyl]amine) were also used to provide insight into the XAS studies of **3**. The reactivity of **3** (–90 °C) has been probed by exposure to a variety of reagents. TMPA causes displacement of the unidentate Me_2im ligands producing **4**, while H^+ liberates H_2O_2 (74%), CO_2 results in the formation of a percarbonato complex ($\lambda_{max} = 350$ nm) which thermally degrades to a carbonato species $[Cu_2(Me_2im)_6(CO_3)]^{2+}$ (**5**), and tertiary phosphines effect the liberation of O_2, yielding $[Cu(Me_2im)_3(PR_3)]^+$ (R = Ph (**6a**); R = Me (**6b**)). The UV–vis spectroscopic properties of **3** and its reactivity suggest that structure **A** is more likely, but considerable additional efforts in the area of Cu_2O_2 structure–spectroscopy–reactivity correlations are needed.

Imidazole ligands (derived from side chain amino acid histidines) are prevalent in the active sites of different copper metalloproteins, including those involved in the binding and activation of dioxygen.[1] Examples include the O_2-carrier hemocyanin[1,2] and copper oxygenases such as tyrosinase[1a,3] and dopamine β hydroxylase[4] as well as copper oxidases such as laccase and ascorbate oxidase,[1a,5] as well as galactose oxidase.[6] Imidazole is also found to be an important donor ligand in iron,[7] zinc,[8] and manganese[9] metalloproteins.

As part of our efforts to contribute to the basic understanding of the chemistry involved in these copper metalloproteins we have been engaged in studying the coordination chemistry of low-coordinate (two, three, and four) copper(I) compounds having nitrogen donor ligands and their reactions with dioxygen.[10] In recent years there has been a significant amount of success in generating and characterizing a number of copper–dioxygen (Cu_2O_2) complexes,[10–14] including two types for which X-ray crystal structures are available. $[\{Cu(TMPA)\}_2(O_2)]^{2+}$ (**4**) (TMPA = tris[(2-pyridyl)methyl]amine) was shown by X-ray

* To whom correspondence should be addressed.
† The Johns Hopkins University.
‡ Daresbury Laboratory.
§ Oregon Graduate Institute.
• Abstract published in *Advance ACS Abstracts*, October 15, 1993.

(1) (a) Solomon, E. I.; Baldwin, M. J.; Lowery, M. D. *Chem. Rev.* **1992**, *92*, 521–542. (b) *Bioinorganic Chemistry of Copper*; Karlin, K. D., Tyeklár, Z., Eds., Chapman & Hall: New York, 1993. (c) Adman, E. T. *Adv. Protein Chem.* **1991**, *42*, 145–197. (d) Sorrell, T. N. *Tetrahedron* **1989**, *45*, 3–68.

(2) (a) Hazes, B.; Magnusm, K. A.; Bonaventura, C.; Bonaventura, J.; Dauter, Z.; Kalk, K. H.; Hol, W. G. J., *Protein Sci.* **1993**, *2*, 597–619. (b) Magnus, K. A.; Ton-That, H.; Carpenter, J. E. In ref 1b, pp 143–150.

(3) (a) Lerch, K. *Met. Ions Biol. Syst.* **1981**, *13*, 143–186. (b) Robb, D. A. In *Copper Proteins and Copper Enzymes*; Lontie, R., Ed.; CRC: Boca Raton, FL, 1984; Vol. 2, pp 207–241.

(4) (a) Stewart, L. C.; Klinman, J. P. *Annu. Rev. Biochem.* **1988**, *57*, 551–592. (b) Klinman, J. P.; Berry, J. A.; Tian, B. In ref. 1b, pp 151–163. (c) Pettingill, T. M.; Strange, R. W.; Blackburn, N. J. *J. Biol. Chem.* **1991**, *266*, 16996–17003.

(5) Messerschmidt, A.; Ladenstein, R.; Huber, R.; Bolognesi, M.; Avigliano, L.; Petruzzelli, R.; Rossi, A.; Finazzi-Agró, A. *J. Mol. Biol.* **1992**, *224*, 179–205.

(6) (a) Ito, N.; Phillips, S. E. V.; Stevens, C.; Ogel, Z. B.; McPherson, M. J.; Keen, J. N.; Yadav, K. D. S.; Knowles, P. F. *Nature* **1991**, *350*, 87–90.

(7) (a) Howard, J. B.; Rees, D. C. *Adv. Protein Chem.* **1991**, *42*, 199–280. (b) Lippard, S. J. *Angew. Chem., Int. Ed. Engl.* **1988**, *27*, 344. (c) Que, L., Jr.; True, A. E. *Prog. Inor. Chem.* **1990**, *38*, 97. (d) Solomon, E. I.; Zhang, Y. *Acc. Chem. Res.* **1992**, *25*, 343–352.

(8) (a) Christianson, D. W. *Adv. Protein Chem.* **1991**, *42*, 281–355. (b) Vallee, B.; Auld, D. S. *Biochemistry* **1990**, *29*, 5647–5659.

(9) (a) Manganese Redox Enzymes, Pecoraro, V. L., Ed.; Verlag-Chemie: New York, 1992. (b) C. G. Dismukes, In *Bioinorganic Catalysis*; Reedijk, J., Ed.; Marcel Dekker: New York 1992; Chapter 10, pp 317–346.

(10) (a) Karlin, K. D.; Tyeklár, Z.; Zuberbühler, A. D. In *Bioinorganic Catalysis*; Reedijk, J., Ed., Marcel Dekker: New York, 1993; Chapter 9, pp 261–315. (b) Tyeklár, Z.; Karlin, K. D. In ref 1b, pp 277–291. (c) Tyeklár, Z.; Karlin, K. D. *Acc. Chem. Res.* **1989**, *22*, 241–248.

(11) (a) Jacobson, R. R.; Tyeklár, Z.; Farooq, A.; Karlin, K. D.; Liu, S.; Zubieta, J. *J. Am. Chem. Soc.* **1988**, *110*, 3690–3692. (b) Tyeklár, Z.; Jacobson, R. R.; Wei, N.; Murthy, N. N.; Zubieta, J.; Karlin, K. D. *J. Am. Chem. Soc.* **1993**, *115*, 2677–2689.

(12) Karlin, K. D.; Cruse, R. W.; Gultneh, Y.; Farooq, A.; Hayes, J. C.; Zubieta, J. *J. Am. Chem. Soc.* **1987**, *109*, 2668–2679.

(13) (a) Karlin, K. D.; Tyeklár, Z.; Farooq, A.; Haka, M. S.; Ghosh, P.; Cruse, R. W.; Gultneh, Y.; Hayes, J. C.; Toscano, P. J.; Zubieta, J. *Inorg. Chem.* **1992**, *31*, 1436–1451. (b) Blackburn, N. J.; Strange, R. W.; Farooq, A.; Haka, M. S.; Karlin, K. D. *J. Am. Chem. Soc.* **1988**, *110*, 4263–4272.

0002-7863/93/1515-11259$04.00/0

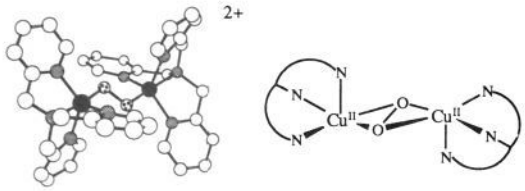

$[\{Cu(TMPA)\}_2(O_2)]^{2+}$ (4) $[Cu(HB(3,5\text{-}iPr_2pz)_3]_2(O_2)$

crystallography to possess a *trans*-μ-1,2-peroxo ligand (ν_{O-O} = 831 cm^{-1}) bridging between two mononuclear copper(II) units.[11] A significant advance has been made by Kitajima and coworkers,[14] who reported the crystallographically characterized compound $[(HB(3,4\text{-}iPr_2pz)_3)Cu]_2(O_2)$, $HB(3,4\text{-}iPr_2pz)_3$ = hydrotris(3,5-diisopropylpyrazolyl)borate) which possesses a planar μ-η^2:η^2-peroxo bridging ligand. This turns out to be the actual structure in oxyhemocyanin (as determined by X-ray crystallography)[2b] and other spectroscopic and physical properties of this compound closely match those found in oxyhemocyanin.[1a,14]

Scheme I

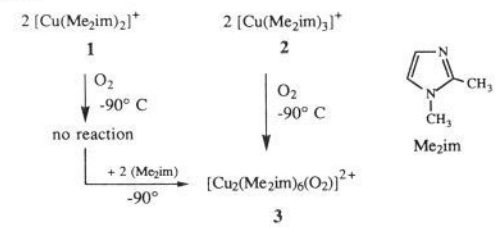

While these aforementioned studies represent important advances in copper biomimetic chemistry, none of these systems has utilized imidazole ligands, the actual donor found in hemocyanin. However, we recently reported the low-temperature generation and preliminary characterization of a new copper–dioxygen (Cu_2O_2) complex using simple unidentate 1,2-dimethylimidazole (L) ligands.[15] Here, we elaborate on chemical and structural aspects of this chemistry (Scheme I). The two-coordinate copper(I) complex $[Cu(Me_2im)_2]^+$ (**1**) has been synthesized and characterized by X-ray diffraction, while this and the three-coordinate species $[Cu(Me_2im)_3]^+$ (**2**) have also been characterized using X-ray absorption spectroscopy (XAS: XANES and EXAFS). XAS has been successfully applied in the extraction of useful structural information for a number of copper protein active sites[16] including those in hemocyanin,[17] laccase,[16,18] dopamine β hydroxylase,[19] superoxide dismutase,[20] and phenylalanine hydroxylase.[21] It is particularly useful as a probe of the otherwise spectroscopically "silent" copper(I) oxidation state, while copper(I) complexes having two, three and four coordination have characteristic edge features which can be differentiated by XANES.[17d,18,21] $[Cu(Me_2im)_3]^+$ (**2**) reacts with dioxygen quasi-reversibly, generating the dinuclear O_2-adduct $[Cu_2(Me_2im)_6(O_2)]^{2+}$ (**3**), for which XAS studies allow the proposal of possibilities for its Cu_2O_2 structure. The chemistry of **3** is also detailed, including its UV–vis spectroscopy, and reactions with H^+, CO_2, CO, PR_3 (R = Ph, Me), and the chelating ligand TMPA.

Experimental Section

Materials and Methods. Reagents and solvents were of commercial quality and were purified according to the published methods.[10b] 1,2-Dimethylimidazole was purified by vacuum distillation (52 °C) and was stored under argon. Preparation, handling, and storage of air-sensitive solids and solutions were carried out under an argon atmosphere by standard methods.[10,13a]

Infrared spectra were recorded as Nujol mulls on a Mattson Galaxy 4030 FT-IR. NMR spectra were measured in CD_3NO_2 or $CDCl_3$ on either a Varian CFT-20 or a Varian XL-400 NMR spectrometer. Room-temperature UV–vis spectra were recorded on a Shimadzu UV-160 spectrophotometer using standard 1-cm quartz cells, while low-temperature spectra were obtained on a Hewlett-Packard 8452A diode array spectrophotometer driven by a Compaq Deskpro 386S computer using a software system written by On-Line Instrument Systems, Inc. Sample preparation and manipulation is as previously described.[11b] EPR spectra were obtained on a Varian E-12 spectrometer (X-band). Room-temperature magnetic moments were determined using a Johnson-Mathey magnetometer calibrated with $Hg[Co(SCN)_4]$, and solution electrical conductivity measurements were obtained in CH_3CN using a Barnstead Model PM-70CB conductivity bridge and YSI Model 3403 cell. Gas chromatographic analyses were carried out on a HP 5890 instrument using a 30-m HP-5 capillary column. Low-temperature manometry (O_2-uptake) was carried out as previously described.[11b] Elemental analyses were performed by Desert Analytics, Tucson, AZ.

Two-Coordinate Complex $[Cu(Me_2im)_2](PF_6)$ ($1(PF_6)$). Under argon, Me_2im (1.0 mL, 11.27 mmol) was dissolved in a mixture of 50 mL of methanol and 10 mL of nitromethane, and this solution was added dropwise with stirring to solid $[Cu(CH_3CN)_4](PF_6)$ (2.10 g, 5.63 mmol) under argon. The solid initially dissolved, and after ~10 min a white precipitate formed. This mixture was stirred under argon for 30 min, at which time all the solvent was evaporated under reduced pressure and the white solid was left to dry under vacuum overnight. The solid was recrystallized from CH_2Cl_2/Et_2O (1:2 by volume) to yield 1.98 g (88%) of white microcrystalline product. Anal. Calcd for $(C_{10}H_{16}CuF_6N_4P)$: C, 29.96; H, 3.98; N, 13.98. Found: C, 29.91; H, 3.68; N, 14.00. ^1H NMR (CD_3NO_2): δ 2.40 (6 H, s, CH_3), 3.60 (6 H, s, NCH_3), 6.85–6.95 (4 H, br d). IR (Nujol): 1620 (C=C, s), 840 (PF_6^-, s, br) cm^{-1}.

Three-Coordinate Complex $[Cu(Me_2im)_3](PF_6)$ ($2(PF_6)$). This was prepared in an identical manner as the two-coordinate complex $1(PF_6)$ by mixing 1,2-dimethylimidazole (1.25 mL, 14.10 mmol) and $[Cu(CH_3CN)_4](PF_6)$ (1.75 g, 4.70 mmol) under an argon atmosphere. An off-white microcrystalline solid (2.12 g, 91%) was finally isolated. Anal. Calcd for $(C_{15}H_{24}CuF_6N_6P)$: C, 36.24; H, 4.88; N, 16.92. Found: C, 36.67; H, 5.11; N, 16.97. ^1H NMR (CD_3NO_2): δ 2.40 (9 H, br s, CH_3), 3.75 (9 H, s, NCH_3), 6.80–7.20 (6H, br). IR (Nujol): 1620 (C=C, s), 840 (PF_6^-, s, br) cm^{-1}.

X-ray Crystallography and Reduction of Diffraction Data. The structure analysis of complex $1\text{-}PF_6$ was performed by Molecular Structure Corporation, Houston, TX. A dichloromethane/diethyl ether solution of compound $2(PF_6)$ under Ar at room temperature yielded colorless plate crystals of $[Cu(Me_2im)_2](PF_6)$ ($1(PF_6)$) suitable for X-ray crystallographic analysis. A crystal having approximate dimensions of 0.300 × 0.350 × 0.100 mm was mounted on a glass fiber. All measurements were made on a Rigaku AFC6R diffractometer with graphite monochromated Mo Kα radiation (λ(Mo Kα) = 0.710 73 Å)

(14) (a) Kitajima, N.; Fujisawa, K.; Fujimoto, C.; Moro-oka, Y.; Hashimoto, S.; Kitagawa, T.; Toriumi, K.; Tatsumi, K.; Nakamura, A. *J. Am. Chem. Soc.* **1992**, *114*, 1277–1291. (b) Kitajima, N.; Fujisawa, K.; Moro-oka, Y.; Toriumi, K. *J. Am. Chem. Soc.* **1989**, *111*, 8975–8976.

(15) Sanyal, I.; Strange, R. W.; Blackburn, N. J.; Karlin, K. D. *J. Am. Chem. Soc.* **1991**, *113*, 4692–4693.

(16) (a) Scott, R. A.; Eidness, M. K. *Comments Inorg. Chem.* **1988**, *7*, 235–267. (b) Blackburn, N. J. In *Synchroton Radiation and Biophysics*; Hasnain, S. S.; Ed.; Ellis Horwood Ltd.: Chichester, U. K., 1990; pp 63–103. (c) Hasnain, S. S. In *Synchroton Radiation and Biophysics*; Hasnain, S. S., Ed.; Ellis Horwood Ltd.: Chichester, UK, 1990; pp 176–200. (d) Feiters, M. C. *Comments Inorg. Chem.* **1990**, *11*, 235–267.

(17) (a) Brown, J. M.; Powers, L.; Kincaid, B. M.; Larabee, J. A.; *J. Am. Chem. Soc.* **1980**, *102*, 4210–4216. (b) Co, M. S.; Hodgson, K. O.; Eccles, T. K.; Lontie, R. *J. Am. Chem. Soc.* **1981**, *103*, 984–986. (c) Co, M. S.; Scott, R. A.; Hodgson, K. O. *J. Am. Chem. Soc.* **1981**, *103*, 986–988. (d) Blackburn, N. J.; Strange, R. W.; Reedijk, J.; Volbeda, A.; Farooq, A.; Karlin, K. D.; Zubieta, J. *Inorg. Chem.* **1989**, *28*, 1349–1357. (e) Volbeda, A.; Feiters, M. C.; Vincent, M. G.; Bouwman, F.; Dobson, B. R.; Kalk, K. H.; Reedijk, J.; Hol, W. G. J. *Eur. J. Biochem.* **1989**, *181*, 669–673.

(18) Kau, L. S.; Spira-Solomon, D. J.; Penner-Hahn, J. E.; Hodgson, K. O.; Solomon, E. I. *J. Am. Chem. Soc.* **1987**, *109*, 6433–6442.

(19) (a) Hasnain, S. S.; Diakun, G. P.; Knowles, P. F.; Binsted, N.; Garner, C. D.; Blackburn, N. J. *Biochem. J.* **1984**, *221*, 545–548. (b) Scott, R. A.; Sullivan, R. J.; DeWolfe, W. E.; Dolle, R. E.; Kruse, L. I. *Biochemistry* **1988**, *27*, 5411–5417. (c) Blumberg, W. E.; Desai, P. R.; Powers, L.; Freedman, J. H.; Villafranca, J. J. *J. Biol. Chem.* **1989**, *264*, 6029–6032. (d) Blackburn, N. J.; Hasnain, S. S.; Pettingill, T. M.; Strange, R. W.; *J. Biol. Chem.* **1991**, *266*, 23120–23127. (e) Blackburn, N. J. In ref 1b, pp 164–183.

(20) (a) Blackburn, N. J.; Hasnain, S. S.; Binsted, N.; Diakun, G. P.; Garner, C. D.; Knowles, P. F. *Biochem. J.* **1984**, *219*, 985–990. (b) Blackburn, N. J.; Strange, R. W.; McFadden, L. M.; Hasnain, S. S. *J. Am. Chem. Soc.* **1987**, *109*, 7162–7170.

(21) Blackburn, N. J.; Strange, R. W.; Carr, R. T.; Benkovic, S. J. *Biochemistry* **1992**, *31*, 5298–5303.

Table I. Two-Coordinate Cu(I) Complexes with Nitrogen Donor Ligands[a]

compound	Cu–N(1), Å	Cu–N(2), Å	N(1)–Cu–N(2), ± deg	ref
$[Cu_2(EDTB)](ClO_4)_2$	1.869(4)	1.876(4)	170.9(1)	24a,c
$[Cu_{12}(C_4H_5N_2S)_{12}(MeCN)_4]][BPh_4]_2(MeCN)_4$	1.867(8)	1.885(8)	179.2(5)	23d
$[Cu(BBDHp)](PF_6)_{0.66}(BF_4)_{0.34}$	1.918(4)		168.5(1)	24c
$[Cu(xyPz)]_2(BF_4)_2$	1.873(4)	1.875(4)	159.7(2)	24b
$[Cu(1\text{-}Mepz)_2](BF_4)$	1.873(3)	1.879(3)	1.78.2(2)	23e
$[Cu(1,3,5\text{-}Me_3pz)_2](BF_4)$	1.878(3)	1.863(4)	173.8(2)	23e
$[Cu(2,4\text{-}Me_2py)_2](ClO_4)$	1.860(1)		170.0(1)	23f
$[Cu_5(mac)_2(dmt)_2](ClO_4)_3$	1.85(3)			24d
$[Cu(2,6\text{-}Me_2py)_2](ClO_4)$	1.879(16)	1.953(22)	171.0(7)	23g
$[Cu(2,6\text{-}Me_2py)_2](PF_6)$	1.898(5)		177.3(2)	23i
$[Cu(1\text{-}Meim)_2](BF_4)$	1.863(7)	1.855(7)	173.6(3)	23h
$[Cu(2,4,6\text{-}Me_3py)_2](BF_4)$	1.900(5)		173.2(3)	23i
$[Cu(1,2\text{-}Me_2im)_2](PF_6)$ (**1**)	1.865(8)		179.2(7)	this work

[a] Key: EDTB, *N,N,N',N'*-tetrabis(2'-benzimidazolylmethyl)-1,2-ethanediamine; $C_4H_5N_2S$, 1-methyl-2-mercaptoimidazole anion; BBDHp, 1,7-bis(2-benzimidazolyl)-2,6-dithiaheptane; xyPz, α,α'-bis(3,4-dimethylpyrazolyl)-*m*-xylene; mac, N_4O_2 macrocyclic ligand; dmt, 3,5-dimethyl-1,2,4-triaazolate anion; Mepz, methyl-substituted pyrazole; Me_npy, methyl-substituted pyridine; Me_nim, methyl-substituted imidazole.

Table II. Crystallographic Data for $[Cu(Me2im)_2](PF_6)$ (**1**(PF_6))

formula	$C_{10}H_{16}CuN_4PF_6$	D_{calcd}, g/cm^3	1.707
temp, °C	−120	space group	*C*2/*c*
cryst syst	monoclinic	no. of reflcns collcd	1119
a, Å[a]	14.877(2)	no. of indep. reflcns	1071
b, Å	15.950(4)	abs coeff, cm^{-1}	1.28
c, Å	6.931(4)	no. refined params (NV)	103
β, deg	108.54(2)	largest peak/hole, eÅ^{-3}	+1.66/−0.58
V, Å^3	1559(1)	R^b	0.067
MW	400.77	R_w^c	0.075
F(000)	808	goodness of fit[d]	2.87
Z	4		

[a] All calculations were performed using the TEXSCAN-TEXRAY Structure Analysis Package, Molecular Structure Corp., 1985. [b] $R = \Sigma[|F_o| - |F_c|/\Sigma|F_o|]$. [c] $R_w = [\Sigma' w(|F_o| - |F_c|)^2/\Sigma w|F_o|^2]^{1/2}$; $w = 1/\sigma^2(F_o) + g^*(F_o)^2$; $g = 0.001$. [d] GOF $= [\Sigma\, w(|F_o| - |F_c|)^2/(NO - NV)]^{1/2}$, where NO is the number of observations and NV is the number of variables.

and a 12 kW rotating anode generator. Cell constants and an orientation matrix for data collection, obtained from a least-squares refinement using the setting angles of 25 carefully centered reflections in the range $35.15 < 2\theta < 42.21°$ corresponded to a monoclinic cell with dimensions shown in Table II.

The data were collected at a temperature of −120 + 1 °C using the ω scan technique to a maximum 2θ value of 45.1°. The ω scans of several intense reflections, made prior to data collection, had an average width at half-height of 0.41° with a take-off angle of 6.0°. Scans of (2.50 + 0.30 tan θ)° were made at a speed of 32.0°/min. Of the 1119 reflections which were collected, 1071 were unique (R_{int} = 0.049). The intensities of three representative reflections which were measured after every 150 reflections remained constant throughout data collection indicating crystal and electronic stability. A summary of cell parameters, data collection parameters, and refinement results is given in Table II.

Structure Solution and Refinement. The structure was solved by direct methods.[22] The non-hydrogen atoms were refined anisotropically. The final cycle of full-matrix least-squares refinement was based on 675 observed reflections ($I > 3.00\ \sigma(I)$) and 103 variable parameters. The standard deviation of an observation of unit weight was 2.87. Neutral atom scattering factors were taken from Cromer and Waber. Anomalous dispersion effects were included in F_{calc}. All calculations were performed using the TEXSAN crystallographic software package from the Molecular Structure Corp. The final *R* factors and refinement data are given in Table II. Tables giving full details of the experimental procedures, positional and thermal parameters, complete bond lengths and angles are given as supplementary material, pp S1–S8.

Reaction of $[Cu_2(Me_2im)_6(O_2)]^{2+}$ (3) with TMPA. Quantification of Peroxide Transfer Reaction by UV–Vis Spectroscopy. Under argon, a solution of the complex $[Cu(Me_2im)_3](PF_6)$ (**2**(PF_6)) (0.0060 g, 1.208×10^{-5} mol) was made in 4.2 mL of CH_2Cl_2 (concentration = 2.87 mM) inside a cuvette assembly as described above. The cuvette was cooled to −90 °C in a liquid N_2/methanol bath and an initial spectrum was recorded. Dry dioxygen was then bubbled through the solution at −90 °C until the color of the solution changed to brown and a spectrum was recorded. The spectrum of this solution was monitored for ~20 min to ensure full formation of the dioxygen complex **3**. Meanwhile, a solution of TMPA (tris[2-(pyridyl)methyl]amine) (0.010 g, 3.448×10^{-5} mol) was made in 40 mL of CH_2Cl_2 under Ar in a 50-mL Schlenk flask fitted with a side arm. This flask was cooled to −90 °C in a liquid N_2/methanol slush bath. Once the formation of **3** was complete, the cuvette assembly was attached to a vacuum line and excess oxygen was removed by repeated vacuum/Ar cycles while vigorously shaking the cuvette. Once all the excess O_2 was removed, under Ar, the stoppers on both the cuvette and the Schlenk flask were changed to rubber septa, and the TMPA solution was transferred to the cuvette assembly using a long needle serving as a cannula. During this process a slight vacuum had to be applied on the cuvette end to assist a faster transfer of the TMPA solution into the cuvette. After most of the TMPA solution was transferred, the cuvette was shaken to mix the two reactants, and an immediate color change to deep purple occurred. A final spectrum of this purple solution was recorded and was similar to $[\{Cu(TMPA)\}_2(O_2)]^{2+}$ (**4**). The percent conversion was calculated on the basis of the extinction coefficient of the peak at 525 nm and comparison to an authentic sample of **4** and was 81%. This experiment was repeated and consistent result was obtained.

Protonation of $[Cu_2(Me_2im)_6(O_2)]^{2+}$ (3): Quantitative Determination of Hydrogen Peroxide Formation by Iodometric Titration. A solution of $[Cu(Me_2im)_3](PF_6)$ (**2**(PF_6)) (0.220 g, 0.443 mmol) was made in 25 mL of CH_2Cl_2 under and was bubbled with dry dioxygen for 5 min at −90 °C to form **3**. This solution was stirred at −90 °C for 20 min at which point excess O_2 was removed by repeated vacuum/Ar purgings. To the brown solution under argon an excess of $HBF_4{\cdot}Et_2O$ (0.488 g, 3.012 mmol) was added with a plastic syringe, and an immediate color change to blue occurred. This solution was stirred for 20 min and an excess of diethyl ether (150 mL) was added dropwise under argon to precipitate the Cu(II) product. The precipitate was allowed to settle down and the supernatant was transferred, with a cannula, to a flask containing a solution of KI (1 g) in a degassed mixture of distilled water (20 mL) and acetic acid (10 mL). The blue precipitate was washed with either (50 mL) and the supernatant again transferred to the KI solution. The yellow KI mixture was stirred vigorously for 10 min at room temperature and was then titrated with 0.051 N $Na_2S_2O_3$ until it became colorless. The mixture consumed 6.6 mL of $Na_2S_2O_3$ solution which corresponds to 0.170 mmol of H_2O_2 (77%).

In a second experiment, $HBF_4{\cdot}Et_2O$ (0.51 g, 3.148 mmol) was added to the brown dioxygen complex **3** prepared from 0.200 g (0.403 mmol) $[Cu(Me_2im)_3(PF_6)$ (**2**(PF_6)) at −90 °C. After treatment of the solution as described above, the KI mixture took up 5.8 mL of 0.051 N $Na_2S_2O_3$ corresponding to 0.149 mmol (74%) of H_2O_2.

Reaction of $[Cu_2(Me_2im)_6(O_2)](PF_6)_2$ ($3(PF_6)_2$) with CO_2. Synthesis of $[Cu_2(Me_2im)_6(CO_3)](PF_6)_2$ ($5(PF_6)_2$). A solution of $[Cu(Me_2im)_3](PF_6)$ (**2**(PF_6)) (0.200 g, 0.403 mmol) was made in 15 mL of CH_2Cl_2 under argon and was oxygenated at −90 °C by bubbling with dioxygen to yield a brown solution of $[Cu_2(Me_2im)_6(O_2)](PF_6)_2$ ($3(PF_6)_2$). After removal of the excess oxygen by repeated vacuum/Ar cycles, excess CO_2 was introduced with the aid of a balloon. The color of the solution changed from brown to blue. The blue solution was stirred at −90 °C for an hour and was slowly warmed up to yield a dark green solution with a small amount of green precipitate. The green mixture was stirred overnight and filtered through a medium-porosity frit, and the solvent was evaporated under vacuum. The resulting green solid was washed with diethyl ether

(22) Gilmore, C. J. *J. Appl. Crystallogr.* **1984**, *17*, 42–46.

(2 × 20 mL) and was crystallized from CH_2Cl_2/Et_2O (1:4) to yield 0.15 g (71%) of a green microcrystalline solid. Anal. Calcd for $C_{31}H_{48}Cu_2F_{12}N_{12}O_3P_2$: C, 35.32; H, 4.56; N, 15.94. Found: C, 35.24; H, 4.76; N, 15.42. UV–vis [CH_2Cl_2; λ_{max}, nm (ϵ, $M^{-1}cm^{-1}$)]: 360 (1940), 712 (350). IR (Nujol): 840 (vs, PF_6^-), 1255 (w, CO_3^{2-}) cm^{-1}. EPR silent (CH_2Cl_2, 77 K). μ_{RT} = 1.68 μ_B/Cu. Λ_m = 250 Ω^{-1} cm^2 mol^{-1}.

Reaction of $[Cu_2(Me_2im)_6(O_2)](PF_6)_2$ ($3(PF_6)_2$) with CO_2 in the Presence of PPh_3. A solution of **3** was generated by low-temperature (–90 °C) oxygenation of $[Cu(Me_2im)_3](PF_6)$ ($2(PF_6)$) (0.211 g, 0.425 mmol) in 20 mL of CH_2Cl_2. After the solution of **3** was reacted with CO_2 at –90 °C, solid PPh_3 (0.112 g, 0.427 mmol) was added to it. The resulting blue solution was stirred at –90 °C for 6 h and was slowly warmed to room temperature to finally yield a green solution with some green precipitate. After the green solution was filtered through a medium-porosity frit and the solvent was evaporated, a green solid was isolated, which was washed with diethyl ether (2 × 30 mL). GC analysis of the ether supernatant showed a 40:60 mixture of $O{=}PPh_3$:PPh_3 (80% conversion). The green solid was recrystallized from CH_2Cl_2/Et_2O (1:4) and yielded 0.15 g (69%) of **5** that was identified by comparing its IR and UV–vis spectra with those of the authentic sample.

Reaction of $[Cu_2(Me_2im)_6(CO_3)](PF_6)_2$ ($5(PF_6)_2$) with H^+. Complex $5(PF_6)_2$ (0.500 g, 0.474 mmol) was dissolved in 45 mL of CH_2Cl_2 under argon, and with the help of a syringe HPF_6 (60% solution in water) (0.23 g, 0.95 mmol) was added to it to yield a blue solution. Argon was bubbled through the solution, and the evolved gas was passed through a saturated solution of $Ba(OH)_2$ for 1 h. The white solid formed was filtered on a sintered crucible, washed with water, and dried overnight at 130 °C to yield 0.055 g (0.279 mmol, 58%) of $BaCO_3$.

Qualitative Determination of Dioxygen Liberation from the Reaction of $[Cu_2(Me_2im)_6(O_2)](PF_6)_2$ ($3(PF_6)_2$) with PPh_3 or PMe_3. A solution of $[Cu(Me_2im)_3](PF_6)$ ($2(PF_6)$) (0.350 g, 0.705 mmol) in 25 mL of CH_2Cl_2 under Ar was oxygenated at –90 to give $3(PF_6)_2$. A bent Schlenk storage tube furnished with a side-arm and filled with solid triphenylphosphine (0.190 g, 0.073 mmol) was carefully attached on top of the Schlenk flask containing $3(PF_6)_2$, to avoid PPh_3 dropping in the oxygenated solution. The sidearm of the storage tube was attached, by means of a rubber tubing, to another Schlenk flask fitted on top with an addition funnel filled with aqueous alkaline pyrogallol solution. The pyrogallol test solution was prepared as follows: potassium hydroxide (10 g) was dissolved in 50 mL of distilled water which had been boiled for 2 h; the hot solution was transferred to the addition funnel and bubbled with Ar for 30 min. The aqueous KOH solution was then added to 1 g of pyrogallol in the attached Schlenk flask. A clear, colorless solution formed which was returned to the addition funnel by inverting the apparatus. With this system, copper solution in the reaction flask could be bubbled with Ar and swept into the pyrogallol test solution.

Excess dioxygen from the brown solution of $3(PF_6)_2$ in the reaction flask was removed by repeated vacuum/Ar purgings. To confirm that there was no excess O_2, Ar was bubbled through the solution, this was passed through the pyrogallol test solution in the addition funnel for 15 min. No color change was observed. After 15 min, PPh_3 was added in the brown solution by slowly tapping the storage tube while sweeping the solution with argon through the test solution. Slowly, over a period of 1 h, the color of the solution faded to a light blue and the pyrogallol test solution changed to a deep brown color, testing positive for the oxygen liberated. When the solution was slowly warmed to room temperature, the pyrogallol solution took an even deeper color.

A similar experiment with trimethylphosphine was performed in a slightly different fashion. A reaction vessel containing a 14/20 female joint, a ⅋ 14/35 male joint and a side arm was used to make the dioxygen complex **3**. The ⅋ 14/35 male joint was attached with the aid of a ⅋ 14/35 female adapter to the addition funnel setup containing the pyrogallol solution. After the copper(I) complex solution was oxygenated and the excess oxygen removed as described above, the glass stopper on the reaction vessel was changed to a rubber septum. A 1 M solution of PMe_3 in THF was injected inside the reaction vessel using a Hamilton gastight syringe. The reaction was fast and within 15 min color of the pyrogallol test solution changed to light blue with concurrent fading of the brown dioxygen complex solution.

Reaction of $[Cu_2(Me_2im)_6(O_2)](PF_6)_2$ ($3(PF_6)_2$) with PPh_3. Synthesis of $[Cu(Me_2im)_3(PPh_3)](PF_6)$ ($6a(PF_6)$). A solution of $[Cu(Me_2im)_3](PF_6)$ ($2(PF_6)$) (0.340 g, 0.685 mmol) was made in 30 mL of dry CH_2Cl_2 under Ar, cooled to –90 °C and oxygenated to yield a brown solution of **3**. After removal of excess O_2 by vacuum/Ar purging, triphenylphosphine (0.190 g, 0.724 mmol) was added to the brown solution. A small flow of argon was passed through the reaction flask to carry out any liberated O_2. The mixture was stirred at –90 °C for 3 h during which time the color of the solution faded to light blue. This solution was slowly warmed up to room temperature and was stirred overnight. To the light blue solution 30 mL of Et_2O was added to precipitate out 80 mg of a Cu(II) impurity, and the mixture was filtered through a medium-porosity frit to yield a light yellow solution. Solvent was removed from the solution by application of a vacuum and the resulting solid was washed with ether (3 × 30 mL) and recrystallized from CH_2Cl_2/Et_2O (1:5 v/v) to yield 0.310 g (67%) of a white microcrystalline solid. GC analysis of supernatant indicated that a minor amount (6.6%) of $O{=}PPh_3$ formed. Anal. Calcd for $C_{33}H_{39}CuF_6N_6P_2$: C, 52.16; H, 5.13; N, 11.06. Found: C, 51.51; H, 5.12; N, 10.76. ^1H NMR (CD_3NO_2): δ 2.10 (9H, br s, CH_3), 3.60 (9H, s, NCH_3), 7.00–7.70 (21H, m) IR (Nujol): 840 (PF_6^-, vs) cm^{-1}.

Reaction of $[Cu_2(Me_2im)_6(O_2)](PF_6)_2$ ($3(PF_6)_2$) with PMe_3. Synthesis of $[Cu(Me_2im)_3(PMe_3)](PF_6)$ ($6b(PF_6)$). A solution of $[Cu(Me_2im)_3](PF_6)$ (**2**) (0.21 g, 0.41 mmol) was made in 20 mL CH_2Cl_2 under Ar. This solution was cooled to –90 °C and O_2 was bubbled for 5 min to generate a deep brown solution. The brown solution was stirred at –90 °C for 10 min and excess dioxygen was removed by bubbling the solution with Ar. Trimethylphosphine (1 M in toluene) (0.46 mL, 0.46 mmol) was added to the brown solution with a Hamilton gastight syringe. The color of the solution slowly faded to a light blue over a period of 1 h at –90 °C. The light blue mixture was slowly warmed up to room temperature, and overnight stirring gave a colorless solution. A white solid was isolated by addition of 80 mL of Et_2O and recrystallized from CH_2Cl_2/Et_2O (1:3 v/v) to yield 0.19 g (81%) of a white microcrystalline solid. Anal. Calcd for $C_{18}H_{33}CuF_6N_6P_2$: C, 37.69; H, 5.76; N, 14.66. Found: C, 37.43; H, 5.59; N, 14.76. ^1H NMR (CD_3NO_2): δ 1.40 (9 H, s, $P(CH_3)_3$), 2.50 (9H, s, CH_3), 3.70 (9H, s, NCH_3), 7.00 (6 H, br) IR (Nujol): 840 (PF_6^-, vs) cm^{-1}.

Preparation of Samples for XAS Measurements. The EXAFS cell used for studying the dioxygen complex **3** consisted of a gold-plated copper cell having a rectangular aperture (22 × 3 mm^2) fitted with 10-μm mylar windows. The dioxygen complex **3** was prepared and transferred to the EXAFS cell in a single operation as follows. The three-coordinate complex **2** (50–60 mg) was dissolved in 3 mL of deoxygenated CH_2Cl_2 in a small glass tube with a sidearm connected to the EXAFS cell via a 18 G syringe needle. The other end of the cell was connected through a 3-way valve to the argon and dioxygen lines. The colorless solution and the EXAFS cell were chilled to –78 °C by immersing those in powdered dry ice and were further cooled to –90 °C by adding a little liquid N_2 over dry ice. Once the solution was cold, dioxygen was introduced into the tube via the valve and the solution was bubbled with O_2 for 5 min to generate the brown dioxygen complex **3**. The oxygenated solution was then transferred to the EXAFS cell by application of a slight positive pressure to the apparatus. The cell was then promptly frozen in liquid nitrogen and stored at 77 K until use (2 days).

The EXAFS sample for $[\{Cu(TMPA)\}_2(O_2)](PF_6)_2$ (**4**) was prepared in a slightly different fashion. Before addition of the Cu(I) precursor $[Cu(TMPA)(CH_3CN)](PF_6)$,[11] the solvent in the reaction tube (CH_2Cl_2) was bubbled with O_2 and chilled with dry ice. The solid was then added quickly and the solution was bubbled for 2 min with O_2 followed by its transfer to the EXAFS cell as described above.

EXAFS Data Collection and Analysis. Samples were measured on beamline X9A at NSLS, Brookhaven National Laboratory, with an electron beam energy of 2.5 GeV and a maximum stored current of 220 mA. The data were collected with a Si(111) double crystal monochromator and a grazing incidence mirror to reject harmonics. Samples of the complexes $[Cu_2(Me_2im)_2(O_2)]^{2+}$ (**3**) and $[\{Cu(TMPA)\}_2(O_2)](PF_6)_2$ (**4**) were measured as frozen glasses in dichloromethane at 100 K in fluorescence mode using a 13-element Ge detector. Energy calibration was achieved by setting the first inflection point of a copper foil spectrum to 8980.3 eV. For EXAFS measurements, the exit slit was set to 1.0 mm, and the resolution was estimated to be about 3 eV by inspection. For edge studies, a 0.2 mm slit-width was employed, giving an estimated resolution of 1 eV. EXAFS data reduction and analysis were performed as described below, using curved wave multiple scattering calculations[30,31] and restrained refinement methods[16c,19d] which allow the imidazole ligands to be simulated as geometrically invariant groups. The complete parameter sets, including the parameters which will define the internal geometry of the imidazole rings are given for each simulation in Tables S9–S20 of the Supplementary Material. The quality of the fits was determined using a least squares fitting parameters or fit index, F, defined

as

$$F^2 = (1/N)\sum k^6(\chi_i^{theor} - \chi_i^{exp})^2$$

Results and Discussion

Synthesis of Copper(I) Complexes. There are relatively few examples of two-coordinate copper(I) complexes with nitrogen ligands, and these are listed in Table I.[23,24] They all possess linear or near-linear coordination geometries. Sorrell has described several of these having substituted pyrazole or imidazole ligand donors,[23e] while Lewin and co-workers reported such complexes containing substituted pyridine or quinoline ligands.[23b] The two-coordinate complex $[Cu(Me_2im)_2](PF_6)$ (**1**) was synthesized by a slight modification of Sorrell's method[23e] by the stoichiometric reaction of 1,2-dimethylimidazole and $Cu(CH_3CN)_4(PF_6)$ in a mixture of methanol and nitromethane. The next important step was to evaporate all the solvent under reduced pressure before recrystallization from CH_2Cl_2/Et_2O to ensure the removal of all the acetonitrile from the system; otherwise the starting material $Cu(CH_3CN)_4(PF_6)$ was reformed in competition with **1**. The colorless solid product is air-stable for long periods and at temperatures <0 °C, it does not react with dioxygen in solution.

Examples of three-coordinate copper(I) compounds having all three ligands as unidentate are relatively scarce. Among these, there are a few examples having sulfur and oxygen donor groups[25] but these will not be discussed here. With nitrogen donors, Lewin has reported a series of complexes utilizing substituted pyridines as ligands.[26] One of these, tris(2-picoline)copper(I) cation, has been characterized by X-ray crystallography and has a distorted trigonal coordination geometry.[26] Recently, a number of three-coordinate complexes with unidentate alkylpyridine ligands have been reported by Habiyakare *et al.*[27] Most of these complexes are in a distorted trigonal environment. For the present study, the three-coordinate tris(1,2-dimethylimidazole)copper(I) compound $[Cu(Me_2im)_3](PF_6)$ (**2**(PF_6)) was synthesized in manner identical to that of **1**, by the stoichiometric addition of the ligand to the copper(I) precursor. By contrast to the two-coordinate species $[Cu(Me_2im)_2](PF_6)$ (**1**(PF_6)), complex **2** is extremely air-sensitive as a solid and in solution.

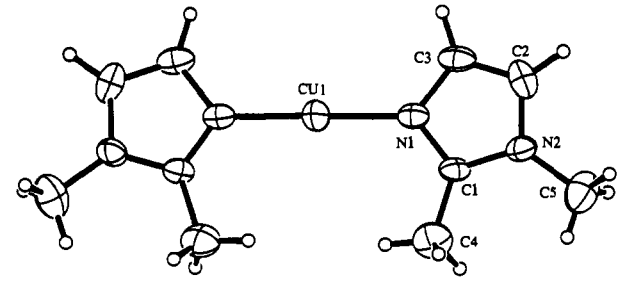

Figure 1. ORTEP diagram of the two-coordinate complex $[Cu(Me_2im)_2](PF_6)$ (**1**), showing the atom labeling scheme.

Structure Description of $[Cu(Me_2im)_2](PF_6)$ (1**(PF_6)).** Complex **1**(PF_6) crystallized as colorless platelets in the monoclinic space group $C2/c$. Experimental details for the structure solution are given in Table II and an ORTEP view of the cation $\mathbf{1}^+$ is given in Figure 1.

The structure of $[Cu(Me_2im)_2](PF_6)$ (**1**(PF_6)) is typical of the two-coordinate copper(I) complexes having monodentate nitrogen donor heterocyclic ligands (Figure 1 and Table I).[23] Crystallographic symmetry (mirror plane) requires that the two $Cu-N_{im}$ distances be equivalent (1.865(8) Å) and the geometry is nearly linear with ∠N–Cu–N = 179.2(7)°. The cations in solid compound **1** are reasonably well separated with 3.466(2) Å being the nearest neighbor distance between the Cu atom in **1** to Cu of the next molecule. The dihedral angles between the two best least-squares imidazole ring planes is 3.07°, showing their near coplanar orientation. The short Cu–N distances contrast with significantly longer bond lengths seen in three-coordinate Cu(I) complexes (>1.9 Å typically).[28] However, there are several examples where strong Cu–N bonding persists (<1.91 Å) while N–Cu–N angle approaches linearity (158–170°) even in the presence of a third donor ligand.[29] The short Cu–N distances and coplanarity of nitrogen heterocyclic ligands in linear two-coordinate molecules such as **1** has been discussed by Sorrell, in terms of strong copper(I)–ligand σ-overlap.[23e,i]

XAS Studies. In a previous communication,[15] we have reported the preliminary details of the reactivity of $[Cu(Me_2im)_2]^+$ (**1**). This two-coordinate complex is unreactive toward either CO or O_2, but reacts stoichiometrically with 1 mol of 1,2-dimethylimidazole to produce the three-coordinate complex $[Cu(Me_2im)_3]^+$ (**2**), which reacts with O_2 to form a dioxygen adduct **3**. A solution CO adduct $[Cu(Me_2im)_3(CO)]^+$ forms and has been analyzed but will be discussed elsewhere. The dioxygen complex **3**, while only stable below −87 °C is the *first* Cu–peroxo complex to be described which contains only unidentate imidazole ligands. The importance of compounds **1–3** lies in the fact that the reaction chemistry with CO and O_2 mimics that of copper proteins such as hemocyanin[2] and dopamine β hydroxylase,[4] since they model the reactivity of the putative enzymatic Cu(I) sites with respect to (i) imidazole ligation, (ii) two- or three-coordination of the precursor complex, and (iii) carbon monoxide binding. XAS spectroscopy is used for the structural characterization of the reaction chemistry involving **1–3**, since we have been thus far unable to obtain X-ray quality crystals for complexes **2** and **3**.

EXAFS of $[Cu(Me_2im)_2](PF_6)$ (1**(PF_6)).** As with previous studies on dioxygen complexes from our laboratories, EXAFS studies on a crystallographically characterized complex (in this case **1**) have been undertaken so as to provide a firm basis for the interpretation of the EXAFS of the noncrystalline complexes (**2** and **3**). The EXAFS of imidazole-containing complexes and proteins exhibits strong peaks in the second and third shells in the Fourier transforms arising from scattering from imidazole

(23) (a) Okkersen, H.; Groeneveld, W. L.; Reedijk, J. *Recl. Trav. Chim. Pays-Bas* **1973**, *92*, 945–953. (b) Lewin, A. H.; Cohen, I. A.; Michl, R. *J. Inorg. Nucl. Chem.* **1974**, *36*, 1951–1957. (c) Hendriks, H. M. J.; Reedijk, J. *Recl. Trav. Chim. Pays-Bas* **1979**, *98*, 95–100. (d) Agnus, Y.; Louis, R.; Weiss, R. *J. Chem. Soc., Chem. Commun.* **1980**, 867–869. (e) Sorrell, T. N.; Jameson, D. L. *J. Am. Chem. Soc.* **1983**, *105*, 6013–6018. (f) Engelhardt, L. M.; Pakawatchai, C.; White, A. H.; Healy, P. C. *J. Chem. Soc., Dalton Trans.* **1985**, 117–123. (g) Munakata, M.; Kitagawa, S.; Shimono, H.; Masuda, H. *Inorg. Chim. Acta* **1989**, *158*, 217–220. (h) Tan, G. O.; Hodgson, K. O.; Hedman, B.; Clark, G. R.; Garrity, M. L.; Sorrell, T. N. *Acta Crystallogr.* **1991**, *C46*, 1773–1775. (i) Habiyakare, A.; Lucken, E. A. C.; Bernardinelli, G. *J. Chem. Soc., Dalton Trans.* **1991**, 2269.

(24) Linear two-coordinate copper (I) complexes having chelating ligands are also known but the two copper ion ligands come from different ligand molecules. See (a) Hendriks, H. M. J.; Birker, P. J. M. W. L.; van Rijn, J.; Verschoor, G. C.; Reedijk, J. *J. Am. Chem. Soc.* **1982**, *104*, 3607–3617. (b) Sorrell, T. N.; Jameson, D. L. *J. Am. Chem. Soc.* **1982**, *104*, 2053–2054. (c) Schilstra, M. J.; Birker, P. J. M. W. L.; Verschoor, G. C.; Reedijk, J. *Inorg. Chem.* **1982**, *21*, 2637–2644. (d) Drew, M. G. B.; Yates, P. C.; Jadwiga, T.-C.; McKillop, K. P.; Nelson, S. M. *J. Chem. Soc., Chem. Commun.* **1985**, 262–263.

(25) (a) Eller, P. G.; Corfield, P. W. R. *J. Chem. Soc., Chem. Commun.* **1971**, 105. (b) Fiaschi, P.; Floriani, C.; Pasquali, M.; Chiesi-Villa, A.; Guastini, C. *J. Chem. Soc., Chem. Commun.* **1984**, 888–890. (c) Garner, C. D.; Nicholson, J. R.; Clegg, W. *Inorg. Chem.* **1984**, *23*, 2148–2150.

(26) Lewin, A. H.; Michl, R. J.; Ganis, P.; Lepore, U. *J. Chem. Soc., Chem. Commun.* **1972**, 661–662.

(27) Habiyakare, A.; Lucken, E. A. C.; Bernardinelli, G. *J. Chem. Soc., Dalton Trans.* **1992**, 2591–2599.

(28) (a) Mealli, C.; Arcus, C. S.; Wilkinson, J. L.; Marks, T. J.; Ibers, J. A. *J. Am. Chem. Soc.* **1976**, *98*, 711–718. (b) Sorrell, T. N.; Malachowski, M. R.; Jameson, D. L. *Inorg. Chem.* **1982**, *21*, 3250–3252. (c) Karlin, K. D.; Hayes, J. C.; Gultneh, Y.; Cruse, R. W.; McKown, J. W.; Hutchinson, J. P.; Zubieta, J. *J. Am. Chem. Soc.* **1984**, *106*, 2121–2128.

(29) (a) Dagdigian, J. V.; Mckee, V.; Reed, C. A. *Inorg. Chem.* **1982**, *21*, 1332–1342. (b) Sorrell, T. N.; Malachowski, M. R. *Inorg. Chem.* **1983**, *22*, 1883–1887. (c) Blackburn, N. J.; Karlin, K. D.; Concannon, M.; Hayes, J. C.; Gultneh, Y.; Zubieta, J. *J. Chem. Soc., Chem. Commun.* **1984**, 939–940.

(30) (a) Sanyal, I.; Blackburn, N. J.; Tyeklár, Z.; Karlin, K. D. To be submitted for publication. (b) Sanyal, I. Ph.D. Dissertation, The Johns Hopkins University, 1992.

(31) Strange, R. W.; Blackburn, N. J.; Knowles, P. F.; Hasnain, S. S. *J. Am. Chem. Soc.* **1987**, *109*, 7157–7162.

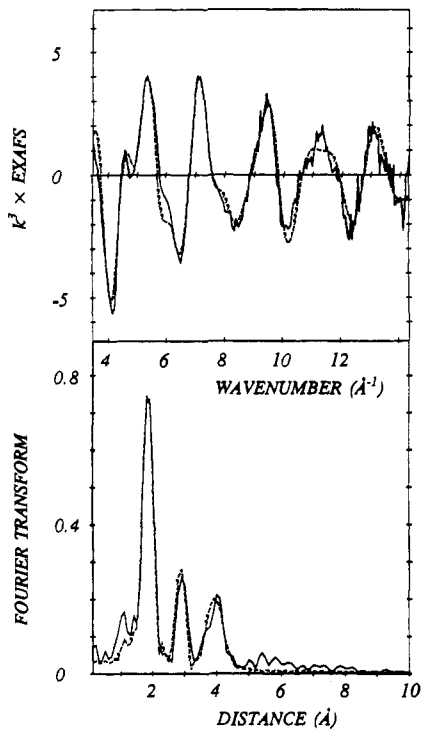

Figure 2. Experimental vs simulated Cu K-EXAFS and Fourier transforms for $[Cu(Me_2im)_2](PF_6)$ (**1**(PF_6)).

ring carbons C2/C5 and C3/N4 ($R \approx 3.0$ Å and 4.1 Å respectively).[16,17,19-21,31a] The associated EXAFS contains contributions from multiple scattering pathways, and as documented in previous publications from our laboratories, can be simulated successfully using the Daresbury program EXCURV,[32] for both models (*tris*- and *tetrakis*(imidazole)copper(II))[31] and imidazole-ligated copper proteins.[19a,d,e,20,21] These analysis procedures have extended the information available from an EXAFS spectrum (over the limited amount available from Fourier filtered first-shell data), and have led to better estimates of the number of coordinated histidine residues. The simulation methods involve constraining the imidazole ligands to be geometrically rigid units using average values of bond lengths and angles determined from crystallographic data on coordination complexes (see ref 19e for a review). In order to test the simulation strategies in the present ligand system, we first carried out a least squares refinement of the EXAFS of **1** using two imidazole groups at the same Cu–N distance, and, as expected due to the presence of crystallographic 2-fold symmetry, a good fit ($F = 0.71$) was obtained with Cu–N = 1.86 Å and outer-shell contributions at the expected radial distances for this value of Cu–N(imid). Figure 2 shows the experimental and simulated EXAFS and Fourier transforms for this fit, with metrical details in Table III. The Debye–Waller terms for the first shell distances are small (0.003 $Å^2$), consistent with identical Cu–N(imid) first-shell distances as required by the crystallographic two-fold symmetry. These parameters agree well with the X-ray crystallographic results (*vide supra*).

EXAFS of $[Cu(Me_2im)_3]^+$ (2). Compound $[Cu(Me_2im)_2]^+$ (**1**) reacts stoichiometrically with 1 equiv of 1,2-dimethylimidazole to produce compound **2**, which analyzes as the *tris* complex $[Cu(Me_2im)_3]^+$ (Scheme I).[15] The EXAFS spectrum of **2**, shown in Figure 3, differs markedly from that of **1** (Figure 2), primarily in the intensity of the first peak in the transform which is approximately 50% less intense than in the *bis* complex **1**. In addition, the first shell appears to be split, as evidenced by the presence of a well-resolved shoulder at *ca* 2.0–2.2 Å. This behavior can only be rationalized by a model involving a distorted 3-coordinate structure with the third ligand binding at a longer distance. The approach to simulating the EXAFS was as follows. The initial parameter set utilized two equivalent imidazole groups with metrical details as found for simulation of **1**, plus an additional imidazole group, to simulate the effect of the third ligand. Least squares fitting gave rise to a well-defined minimum at R1 = 1.89 Å and R2 = 2.08 Å as shown in Figure 3b. Furthermore, the data shows that no other minima exist over the range of Cu–N values from 1.84 to 2.30 Å for either set of imidazole groups. After small adjustments to the ring geometry, the fit shown in Figure 3a was obtained ($F = 0.20$), corresponding to two short (1.89 Å) and one longer (2.08 Å) Cu(I)–N1 interactions. In this case the Debye–Waller term for the longer imidazole is small (0.003 $Å^2$) as expected for a single Cu–N interaction at this distance, but the pair of shorter Cu–N(imid) interactions exhibit larger Debye–Waller terms than found in **1**. This may imply that they, too, are split, but by an amount too small to be resolved by EXAFS. (In general, two Cu–L interactions are discernible by EXAFS only if the splitting, ΔR_{exp}, is larger than the theoretical EXAFS resolution $\Delta R_{theo} \approx \pi/2\Delta k$ where Δk is the fitting range in energy space. In the present case $\Delta R_{theo} = 0.14$ Å. Thus, while the longer Cu–N interaction should clearly be discernible at the resolution of the data, as is evident from the well-resolved splitting for the first shell in the FT, smaller splittings of the shorter Cu–N(imid) pair would appear as an increase in the Debye–Waller term.)

The single deep minimum in the least squares analysis indicates a particularly well-defined structure for **2** as determined by EXAFS. Furthermore, the structure has remarkable similarities to the structures of three-coordinate Cu(I) complexes of tridentate PY2 type ligands (PY2 = bis[2-(2-pyridyl)ethyl]amine) containing two short Cu–N(pyridyl) (1.88–1.94 Å) bonds and one long Cu–N(amine) (2.1–2.3 Å) bond, as determined by X-ray crystallography.[13,17d,29c,33,34] Di- and mononuclear members of this latter class of complexes (e.g. $([Cu_2^I(Nn)]^{2+}$) are known to react with dioxygen to form Cu_2O_2 peroxo-bridged adducts as intermediates on route to oxidation or hydroxylation products and a number of these Cu(II)-peroxo species have been characterized in solution at low temperature (Scheme II).[12,13,33,34]

Adoption of this distorted three-coordinate structure by the Cu(I) complex of the unidentate ligand 1,2-dimethylimidazole is of particular interest, since it implies that constraints other than polydentate ligand connectivity are determining the stereochemistry. One such constraint could be the steric bulk of the methyl groups which might prevent regular trigonal coordination. As a further speculation, it is tempting to propose that the distorted structure in the precursor is important for the stabilization of peroxo adducts, and we note in this regard unsubstituted and other imidazole derivatives (e.g., 1-Meim) do not appear to exhibit analogous chemistry.[30]

Reaction of $[Cu(Me_2im)_2]^+$ (1) and $[Cu(Me_2im)_3]^+$ (2) with Dioxygen at −90° C. A dichloromethane solution of the two-coordinate copper(I) complex $[Cu(Me_2im)_2]^+$ (**1**) does not react with dioxygen at −90 °C (Scheme I, *vide supra*), in accord with earlier findings by Sorrell.[23e] However, addition of an extra equiv of Me_2im to **1** or direct reaction of the three-coordinate complex $[Cu(Me_2im)_3]^+$ (**2**) with O_2 in dichloromethane at −90 °C (conc. ≥ 1.5 mM) promptly gives a brown solution which is stable at −90 to −85 °C for *ca.* 6–7 h. The stoichiometry of the oxygenation reaction was determined manometrically (CH_2Cl_2 at −87 °C), with the observed uptake being $Cu/O_2 = 2.05 \pm 0.05$, indicating

(32) (a) Binsted, N.; Gurman, S. J.; Campbell, J. W. SERC Darsbury Laboratory EXCURV88 Program, Warrington, Cheshire, UK. (b) Gurman, S. J.; Binsted, N.; Ross, I. *J. Phys. C: Solid State Phys.* **1984**, *17*, 143–151. (c) Gurman, S. J.; Binsted, N.; Ross, I. *J. Phys. C: Solid State Phys.* **1986**, *19*, 1845–1861.

(33) (a) Karlin, K. D.; Gultneh, Y.; Hutchinson, J. P.; Zubieta, J. *J. Am. Chem. Soc.* **1982**, *104*, 5240–5242. (b) Karlin, K. D.; Gultneh, Y.; Hayes, J. C.; Cruse, R. W.; McKown, J. W.; Hutchinson, J. P.; Zubieta, J. *J. Am. Chem. Soc.* **1984**, *106*, 2121–2128.

(34) Sanyal, I.; Mahroof-Tahir, M.; Nasir, M. S.; Ghosh, P.; Cohen, B. I.; Gultneh, Y.; Cruse, R. W.; Farooq, A.; Karlin, K. D.; Liu, S.; Zubieta, J. *Inorg. Chem.* **1992**, *31*, 4322–4332.

Table III. Metrical Details of Compounds 1–4 as Determined by EXAFS Where Coordination Numbers Are Given in Parentheses for Each Shell and Unless Otherwise Stated, Estimated Errors in Distances are ± 0.02 Å for the First Shell and ± 0.05 Å for the Outer Shell Interaction

	1		2		3A[a]		3B[b]	
	R	DW[c]	R	DW[c]	R	DW[c]	R	DW[c]
Cu–N (imid)	1.86 (2 N)	0.003	1.89 (2 N)	0.010	2.02 (3 N)	0.004	2.01 (2 N)	0.005
			2.08 (1 N)	0.003			2.24 (1 N)	0.026
Cu–O (peroxo)					1.88 (1 O)	0.002	1.92 (2 O)	0.011
					2.85 (1 O)	0.016		
Cu–Cu							2.84 (1 Cu)	0.018
fit index, *F*	0.71		0.20		1.50		1.33	

[a] Refers to Model **A** for the structure of **3** (Scheme III). [b] Refers to Model **B** for the structure of **3** (Scheme III). [c] Debye–Waller Term ($2\sigma^2$).

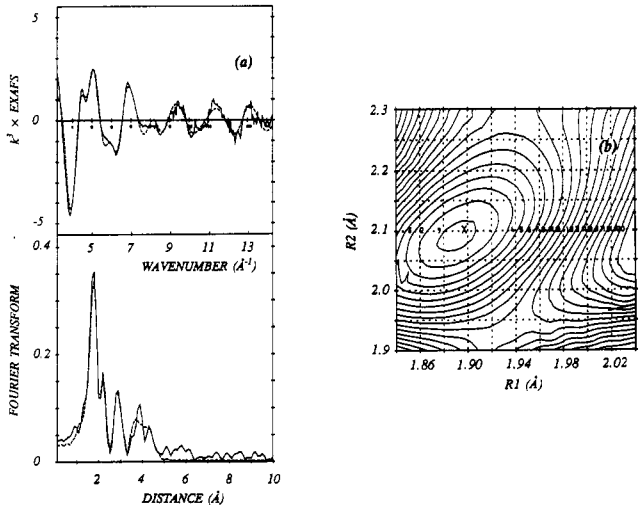

Figure 3. (a) Experimental vs simulated Cu K-EXAFS and Fourier transforms for $[Cu(Me_2im)_3](PF_6)$ (**2**(PF_6)). (b) Contour map of the three-dimensional surface which describes the variation of least-squares fit index (*F*) as a function of the short and long first-shell Cu–N(imid) distances R1 and R2. F_{min} = 0.29 at R1 = 1.90 and R2 = 2.10 Å. The lower contour in the diagram corresponds to *F* = 0.37 and the upper contour to *F* = 6.16. The increment between contours is 0.30. For further details, see text.

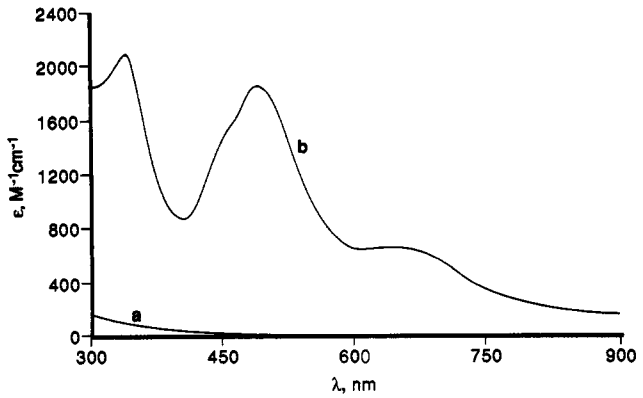

Figure 4. UV–vis spectra of $[Cu(Me_2im)_3]^+$ (**2**) (spectrum **a**) and the dioxygen adduct $[Cu_2(Me_2im)_6(O_2)]^{2+}$ (**3**) (spectrum **b**) in CH_2Cl_2 at –90 °C.

Scheme II

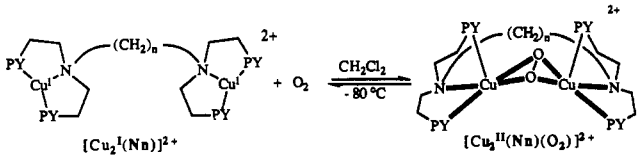

the brown product can be formulated as a peroxodicopper(II) complex, $[Cu_2(Me_2im)_6(O_2)]^{2+}$ (**3**). Solutions generated in this manner are EPR silent, also consistent with the dinuclear formulation with O_2 (peroxo) bridging and antiferromagnetically coupling the two Cu(II) ions. The presence of Cu(II) ion in **3** is also indicated by the XAS measurements, discussed below. We note that an *in situ* mixture of $[Cu(CH_3CN)_4](PF_6)$ and 3 equiv of 1,2-dimethylimidazole in CH_2Cl_2 at –90 °C reacts with O_2 in a similar manner (Cu/O_2 = 2:1, manometry). However, in propionitrile as solvent, **2** does not at all react with dioxygen; this presumably is due to the fact that RCN nitrile groups are strong Cu(I) ligands, and rapid replacement of the unidentate Me_2im copper ion donors would occur under these conditions.

A solution of $[Cu(Me_2im)_3]^+$ (**2**) in dichloromethane (concentration ≥ 1.5 mM) does not show any absorption peak in the UV-vis region (>300 nm), Figure 4, spectrum a. The dioxygen adduct $[Cu_2(Me_2im)_6(O_2)]^{2+}$ (**3**) exhibits multiple absorptions, occuring at 346 (ϵ = 2300 M^{-1} cm^{-1}), *ca.* 450 (sh, ϵ = 1450 M^{-1} cm^{-1}), 498 (ϵ = 2000 M^{-1} cm^{-1}) nm, Figure 4, spectrum b. An additional weaker band is seen at *ca.* 650 nm (sh, ϵ = 680 M^{-1} cm^{-1}) tentatively assigned as a *d–d* transition. The stronger higher energy bands are presumed to be of ligand-to-metal charge-transfer (LMCT) origin, as deduced for other Cu_2O_2 complexes. However, the absorptivity of the vis and near-UV bands is considerably lower than seen for complexes such as [{Cu(TMPA)}$_2(O_2)]^{2+}$ (**4**) and $[Cu_2(Nn)(O_2)]^{2+}$; qualitatively, the spectrum somewhat resembles that for **4** with its end-on bridging *trans*-μ-1,2-peroxo coordination and 440, 525, and 590 nm peroxo-to-Cu(II) LMCT absorptions,[11] but with an additional imidazole-to-Cu(II) LMCT transition, expected at ~350 nm.[35] The lack of an intense band ($\epsilon \sim$ 20 000) in the 340–360-nm region, like that seen in oxyhemocyanin and $[(HB(3,4\text{-}iPr_2pz)_3)Cu]_2(O_2)$, suggests that a *planar* side-on μ-η^2:η^2 is not present. However, firm conclusions concerning spectroscopic assignments obviously cannot be made in the absence of a definitive knowledge of the structure of $[Cu_2(Me_2im)_6(O_2)]^{2+}$ (**3**) (*vide infra*).

While one expects complicated multiple species may form and complex multiple equilibria could be present, our overall observations are consistent with the formation of one predominant species $[Cu_2(Me_2im)_6(O_2)]^{2+}$ (**3**), a Cu/O_2 = 2:1 adduct. As long as the solution concentration of $[Cu(Me_2im)_3]^+$ (**2**) is kept above ~1.5 mM, and the temperature is below –85 °C, the stoichiometry of the O_2 reaction is reproducible and additional Me_2im has no effect on UV–vis spectral features. Preliminary stopped-flow kinetics/spectroscopic studies on analogously generated products using 1-methyl-2-ethylimidazole as the unidentate ligand indicate complex behavior with multiple species present.[36] In the present system, one additional observation of note is that oxygenation of **2** at low concentrations in CH_2Cl_2 (≤1 mM) leads to a blue colored solution (EPR silent) with two absorption bands, λ_{max} = 336 (ϵ = 710 M^{-1} cm^{-1}) and 596 (ϵ = 65 M^{-1} cm^{-1}) nm.[30b] We speculate this could be an intermediate 1:1 Cu/O_2 adduct, like that seen when [{Cu(TMPA)]$^+$ reacts with O_2 to initially produce the mononuclear species [{Cu(TMPA)$(O_2)]^+$.[37]

(35) Schugar, H. J. In *Copper Coordination Chemistry: Biochemical & Inorganic Perspectives*, Karlin, K. D., Zubieta, J., Eds., Adenine Press: Guilderland, NY, 1983; pp 43–74.
(36) Zuberbühler, A. D. In *Bioinorganic Chemistry of Copper*, Karlin, K. D., Tyeklár, Z., Eds., Chapman & Hall: New York, 1993; pp 264–276.
(37) Karlin, K. D.; Wei, N.; Jung, B.; Kaderli, S.; Zuberbühler, A. D. *J. Am. Chem. Soc.*, **1991**, *113*, 5868–5870.

Chart I

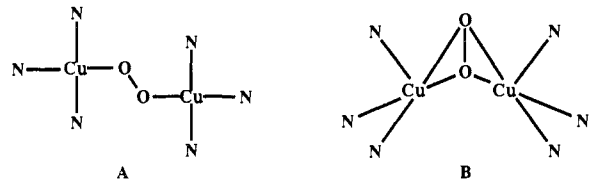

EXAFS of the Dioxygen Adduct $[Cu_2(Me_2im)_6(O_2)]^{2+}$ (3). X-ray absorption edge data (discussed in detail below) show this to be a Cu(II) entity, and the properties discussed above, plus those deduced from chemical reactivity studies (*vide infra*), lead to the conclusion that $[Cu_2(Me_2im)_6(O_2)]^{2+}$ (**3**) is a peroxo-bridged dicopper(II) complex. Reference to the crystal structures of $[\{Cu(TMPA)\}_2(O_2)]^{2+}$ (**4**),[11] $[Cu(HB(3,5\text{-}iPr_2pz)_3)]_2(O_2)$,[14] and oxy-hemocyanin[2b] indicates that either end-on or side-on peroxo bridging may be possible for coordination in a Cu_2O_2 species such as **3**. Solution EXAFS spectroscopic studies and the presence of an intense 360-nm absorption implicated side-on but bent peroxo bridging (i.e., with shorter Cu···Cu distances 3.2–3.4 Å) in species such as $[Cu_2(Nn)(O_2)]^{2+}$ [13b] (Scheme II); in part, these findings led us to consider the side-on peroxo coordination for **3**. Additional precedence for such a bent μ-η^2:η^2-O_2^{2-}-coordination comes from the structure of a vanadium(V) peroxo complex $[\{O(O_2)(F)V\}_2(O_2)F]^{3-}$, with bridging peroxo and F⁻ ligands.[38] Bent disulfur (e.g., formally S_2^{2-}) μ-η^2:η^2 ligation is also well-known in coordination chemistry.[39]

End-on peroxo bonding would result in a maximum of four-coordination at Cu(II) involving one peroxo and three 1,2-dimethylimidazole ligands, whereas side-on bonding would allow five-coordination as the result of η^2-η^2 peroxo bonding. Our EXAFS analysis was designed to test which type of structure was most probable. Initial simulations showed that the first shell amplitude was adequately accounted for by four O/N ligands. Further analysis involving imidazole group fitting examined two models: A ("end-on"; 3 imidazoles + 1 O (peroxo) and B ("side-on"); 2 imidazoles + 2 O (peroxo), Chart I. In B structural considerations would allow the inclusion of an additional imidazole group (or first shell N atom), if this led to a significant improvement in the least squares residual. In A the only additional atom/group which could contribute would be the noncoordinated O atom from the peroxo group. In both cases we also examined the effect of including Cu–Cu scattering to investigate the likelihood of μ-peroxo bridging.

The results of these simulations are shown in Figure 5 (Model A) and Figure 6 (Model B). Model A gave rise to satisfactory agreement between theory and experiment with 3 Cu–N(imid) = 2.01 Å, 1 Cu–O(peroxo) = 1.88 Å, and F = 1.65, although the intensity of the second shell in the transform of the experimental spectrum was found to be too intense relative to that of the third shell (Figure 5a). This could be overcome to some extent by including the uncoordinated O atom as a separate shell at 2.85 Å (F = 1.57, Figure 5b). This is 0.19 Å larger than the position of the uncoordinated O atom in $[\{Cu(TMPA)\}_2(O_2)]^{2+}$ (**4**) in which the peroxo group (Cu–O = 1.85 Å) binds in a *trans* fashion between the two copper ions, which are 4.36 Å apart.[11] For model B, a rather poor simulation was achieved with just 2 Cu–N(imid) = 2.01 Å and 2 Cu–O(peroxo) = 1.92 Å (F = 2.40, Figure 6a), whereas inclusion of an "axial" N atom at 2.24 Å (as conceptually allowed by the model) decreased F to 2.18 (Figure 6b). As anticipated if this shell was indeed derived from an axially coordinated imidazole, the Debye–Waller term was much larger (0.026 Å²). Thus, to this point and in the absence of any Cu–Cu interaction, the data seem to prefer model A (Chart I).

(38) Lapshin, A. E.; Smolin, Y. I.; Shepelev, Y. F.; Schwendt, P.; Gyepesova, D. *Acta Crystallogr.* **1990**, *C46*, 1753–1755.
(39) Hegetschweiler, K.; Keller, T.; Bäumle, M.; Rihs, G.; Schneider, W. *Inorg. Chem.* **1991**, *30*, 4342–4347.

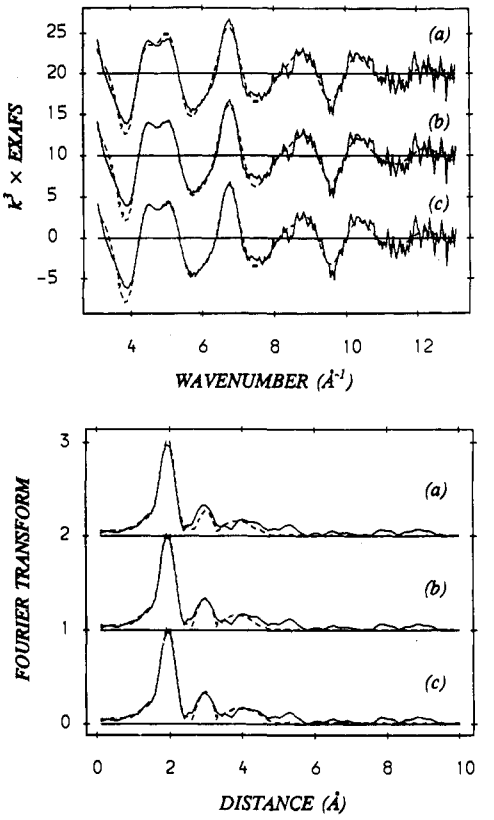

Figure 5. Experimental vs simulated Cu K-EXAFS and Fourier transforms for $[Cu_2(Me_2im)_6(O_2)]^{2+}$ (**3**), model **A**: (a) 3 Cu-N(imid) at 2.01 Å and 1 Cu-O(peroxo) at 1.88 Å: (b) as in a, but including an additional O atom at 2.85 Å; (c) as in b, but including a Cu–Cu interaction at 4.31 Å.

In the absence of data on $\nu_{O=O}$, the oxidation state of the bound dioxygen in $[Cu_2(Me_2im)_6(O_2)]^{2+}$ (**3**) remains uncertain, but as already assumed in the discussion, the reactivity of dioxygen in related systems would suggest a μ-peroxo formulation as a most likely probability. This would introduce a Cu-Cu interaction into each of the above models. In model **A**, both *cis* and *trans* μ-1,2-peroxo bridging is possible and would result in approximate Cu–Cu distances around 3.5–4.0 Å respectively. In model **B**, a planar η^2:η^2 peroxo arrangement would give rise to a Cu–Cu distance of *ca.* 3.5 Å, but shorter Cu–Cu distances are possible if the structure is bent into butterfly configuration, hinged along the O–O bond. The results of including the copper waves in the simulations are shown in Figures 5c and 6c. No improvement in the fit is obtained for model **A** (Figure 5c, F = 1.50) for a Cu wave anywhere in the expected range, *ca.* 3.2–4.5 Å, but the absence of a significant Cu–Cu interaction in **A** in no way excludes this structure, particularly if the peroxo group is bound in a *trans* fashion (see below). For model **B**, a dramatic improvement is obtained for Cu–Cu = 2.84 Å (F = 1.33, Figure 6c) implying a nonplanar η^2:η^2 structure.

EXAFS analysis often suffers from the fact that inclusion of additional shells of atoms with high Debye–Waller terms can sometimes lead to small improvements in the fit, regardless of whether the atoms are really present in the structure. Thus, the uniqueness of the proposed structures depends on the uniqueness of the contribution of the Cu–Cu at 2.84 Å in **B** and to a lesser extent the O at 2.85 Å in **A**. Model compounds exist in which the contributions from both types of interactions can be tested. $[Cu_2(\mu\text{-DMAD})(TC\text{-}6,6)]$ contains a dinucleating tropocoronand macrocycle (TC-6,6) with a μ-η^2:η^2-dimethylacetylene dicarboxylate (DMAD) ligand coordinated between two Cu(I) centers in a bent butterfly configuration.[40] No multiple scattering contributions are expected in this complex as there are no conformationally immobile pathways with interatomic pathways

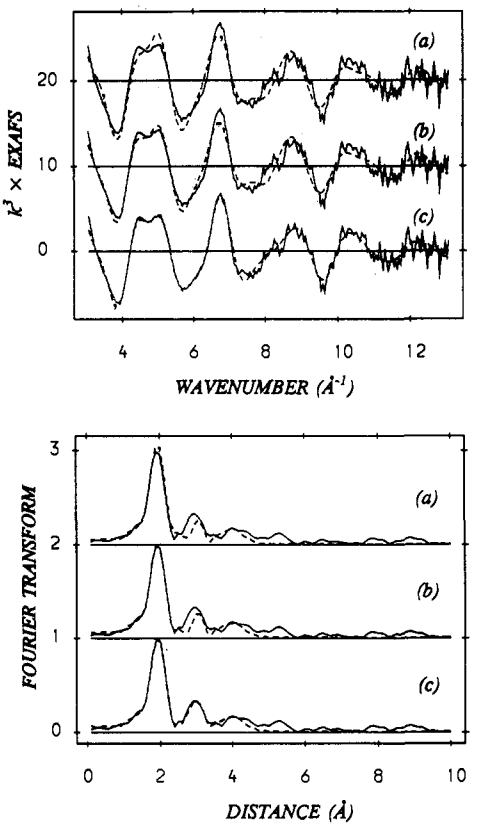

Figure 6. Experimental vs simulated Cu K-EXAFS and Fourier transforms for $[Cu_2(Me_2im)_6(O_2)]^{2+}$ (**3**), model **B**: (a) 2 Cu–N(imid) at 2.01 Å and 2 Cu–O(peroxo) at 1.92 Å; (b) as in a, but including an additional axial N atom at 2.24 Å; (c) as in b, but including a Cu–Cu interaction at 2.84 Å.

in excess of 140°. The Cu–Cu distance is 2.788 Å, with additional shells of 2C and 4C at average crystallographic distances at 2.73 Å and 3.06 Å. EXAFS simulations of this complex show that the second-shell peak can be well fit by a Cu-Cu interaction at the crystallographic distance, but this is in no way a unique fit. Simulations using only C atoms at their expected distances provide numerically equivalent and visually superior fits to the data.[41]

$[\{Cu(TMPA)\}_2(O_2)]^{2+}$ (**4**) contains a *trans* μ-1,2-peroxo bridge between copper atoms 4.3 Å apart. The noncoordinated O atom is 2.66 Å from the Cu and thus provides a model for testing the contribution suggested in model **A**. The EXAFS of **4** can be simulated satisfactorily with four nitrogen ligands at an average distance of 2.05 and one O at 1.85 Å, respectively, in agreement with the X-ray structure.[11] Neither the second peroxo O atom nor the Cu–Cu interaction makes any contribution to EXAFS.[42] These results imply that the additional shells of atoms included in models **A** and **B** can not be considered as uniquely defining either structure. On the other hand, the data cannot exclude their presence. We conclude that either structure is consistent with the data.

Absorption Edges. Figure 7 compares the absorption edges for compounds **1**, **2**, and **3** together with that of $[\{Cu_2(TMPA)\}_2(O_2)]^{2+}$ (**4**). The Cu(I) complexes **1** and **2** exhibit well-resolved edge features at 8984.7 (Figure 7a) and 8984.0 eV (Figure 7b), respectively. The 8984.7-eV peak in **1** can be assigned to the 1s to the nonbonding $4p_{x,y}$ transition of the linear two-coordinate complex.[1a,17d,18] It is evident that this transition is also present

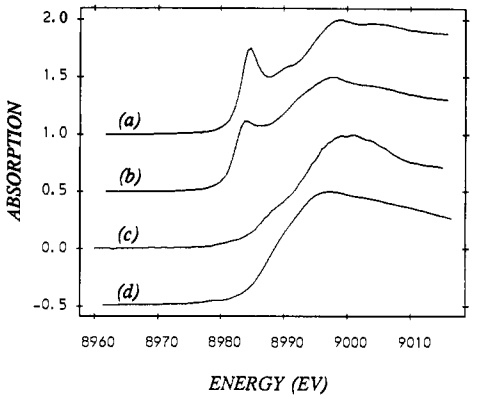

Figure 7. X-ray absorption K-edges for (a) $[Cu(Me_2im)_2](PF_6)$ (**1**(PF_6)), (b) $[Cu(Me_2im)_3](PF_6)$ (**2**(PF_6)), (c) $[Cu_2(Me_2im)_6(O_2)]^{2+}$ (**3**) and (d) $[\{Cu(TMPA)\}_2(O_2)]^{2+}$ (**4**).

in the edge spectrum of **2**, although its intensity is attenuated considerably. This behavior has been noted previously in three-coordinate Cu^1N_3 systems, where the 8984-eV transition has been assigned to a $1s \rightarrow 4p_x$ transition, where the x direction is taken to be normal to the N_3 plane.[18,21] The intensity of the transition is expected to be less than that of the two-coordinate complex, since the presence of only one nonbonding orbital reduces the probability of the transition. However, the intensity has also been observed to correlate with the degree of planarity of the three-coordinate system.[17d] Thus the intensity decreases with the degree of distortion of the complex from planar (trigonal D_{3h} or T-shaped C_{2v}) toward pyramidal (C_{3v}) geometry where the band is generally present only as a shoulder. A simplistic explanation of this effect supposes that distortion from planarity requires increasing amounts of $4s + 4p_z$ mixing in the excited states, and consequently makes the transition increasingly forbidden. These considerations, and comparisons with other published data,[17d,18,21] together with the evidence from EXAFS for two short and one long Cu-N(imid) distances, support a T-shaped geometry in **2**, with minor distortions from planarity.

Parts c and d of Figure 7 show absorption edges for the dioxygen complexes $[Cu_2(Me_2im)_6(O_2)]^{2+}$ (**3**) and $[\{Cu_2(TMPA)\}_2(O_2)]^{2+}$ (**4**). The half-maximal energies of these occur around 8990 eV and confirm their assignment as Cu(II) complexes. Close inspection shows a poorly resolved shoulder at 8986 eV in the edge of **3**. Similar features are often observed in the edge spectra of dinuclear complexes containing tetragonally distorted square pyramidal Cu(II) ions such as $[Cu_2(XYL\text{-}O\text{-})(OH)]^{2+}$ and $[Cu_2(N3)(OMe)_2]^{2+}$, in which the μ-bridging groups occupy equatorial positions.[13b] The edge spectrum of **4** is somewhat different with little or no evidence for resolved edge features. In this case, the Cu coordination is best described as trigonal bipyramidal, with a *trans* μ-1,2-peroxo group bridging along the axial direction. Both edges differ from those of square planar Cu(II) complexes such as $[Cu(imid)_4]^{2+}$ [43] or $CuCl_4^{2-}$,[1a,44] in which well resolved, z-polarized, features are observed at 8986 ± 1 eV. These peaks are usually given the same assignment as the 8984-eV features in the Cu(I) spectra, namely $1s \rightarrow 4p_z$ with the z-direction normal to the CuL_4 plane, where the intensity and strong z-polarization arise from the essentially nonbonding and pure p_z nature of the final state. The attenuation of this peak in the noncentrosymmetric (C_{4v}) five-coordinate complexes may arise from symmetry allowed s–p mixing as suggested for the Cu(I) complexes, although other interpretations involving interligand multiple scattering have also been reported.[43]

The above considerations suggest noncentrosymmetric coordination in $[Cu_2(Me_2im)_6(O_2)]^{2+}$ (**3**), and would appear to rule

(40) Villacorta, G. M.; Gibson, D.; Williams, I. D.; Whang, E.; Lippard, S. J. *Organometallics* **1987**, *6*, 2426–2431.

(41) The experimental versus simulated EXAFS for $[Cu_2(\mu\text{-DMAD})(TC\text{-}6,6)]$ with Cu–Cu and/or Cu–C outer-shell interactions are provided in Tables S18 and S19 of the supplementary material.

(42) The experimental versus simulated EXAFS for $[\{Cu(TMPA)\}_2(O_2)]^{2+}$ (**4**) is provided in Table S17 of the Supplementary Material.

(43) Strange, R. W.; Alagna, L.; Durham, P.; Hasnain, S. S. *J. Am. Chem. Soc.* **1990**, *112*, 4265–4268.

(44) Smith, T. A.; Penner-Hahn, J. E.; Berding, M. A.; Doniach, S.; Hodgson, K. O. *J. Am. Chem. Soc.* **1985**, *107*, 5945–5955.

out square planar geometry based on 3 N(imid) + 1 O(peroxo) ligation, i.e., model A. Other four-coordinate geometries based on trigonal pyramidal or tetrahedral structures could be envisaged, but such structures are rare in Cu(II) chemistry. In reality, Cu(II) has a pronounced preference to achieve five-coordination wherever possible. Examples of this trend include complexes of tetradentate N_4 or N_2S_2 tripodal ligands which form stable Cu(I) complexes, $[CuL]^+$, but when oxidized, coordinate an extra exogeneous ligand to form $[CuLX]^+$.[40] In the absence of exogeneous ligands, the counterion (e.g. nitrate, chloride, sulfate) coordinates strongly (Cu–X ≈ 2.0 Å) to the Cu(II). Both square pyramidal and trigonal bipyramidal complexes are known in this class.[45] The structural chemistry of $[\{Cu(TMPA)\}_2(O_2)]^{2+}$ (**4**) itself follows this rule with $X = O_2^{2-}$. On the other hand, Kitajima's $[Cu(HB(3,5\text{-}iPr_2pz)_3)]_2(O_2)$,[14] in which the pyrazolylborate ligand only provides three donors, adopts the μ-η^2:η^2-peroxo coordination at each copper. We have previously used these arguments to propose μ-η^2:η^2-peroxo coordination in the $[Cu_2(Nn)(O_2)]^{2+}$ series of peroxo complexes (Scheme II),[13b] and we note that the absorption edges of these complexes resembled that of **3** as well as those of the structurally characterized square pyramidal complexes. All these factors argue preferentially for the bent side-on bound peroxo species for $[Cu_2(Me_2im)_6(O_2)]^{2+}$ (**3**), model **B** (Chart I), although the alternative explanation of weak association of the PF_6^- counterion[46] in a pseudoaxial position which might not be detected by EXAFS spectroscopy, remains a possibility.

Reaction Chemistry of $[Cu_2(Me_2im)_6(O_2)]^{2+}$ (3). Reactions of acid, carbon dioxide, tertiary phosphines, phenols, and other reagents with copper–dioxygen complexes have been found to be of considerable use in establishing their nature, For example, reactions of H^+, CO_2 and PPh_3 with $[\{Cu(TMPA)\}_2(O_2)]^{2+}$ (**4**) (with the *trans* μ-1,2-peroxo group) causes nearly quantitative production of H_2O_2, a carbonato–dicopper(II) complex and liberation of dioxygen, respectively. By contrast, exposure of the same reagents under identical conditions to $[Cu_2(Nn)(O_2)]^{2+}$ (with proposed bent side-on μ-η^2:η^2-peroxo coordination, Scheme II) gives no reaction with any of these. The dramatically varying reactivity patterns were previously proposed to be indicative of the very different peroxo ligation in these complexes, the former behaving like a late transition-metal nucleophilic (or basic) peroxo reagent, while the latter being an electrophilic or nonbasic peroxo–metal species.[47] Thus, we subjected $[Cu_2(Me_2im)_6(O_2)]^{2+}$ (**3**) to these same reagents in order to probe the nature of the Cu_2O_2 species formed with the Me_2im imidazole ligand. Furthermore, the unidentate presumably less stable nature of **3** compared to compounds with chelating polydentate ligands suggested to us the idea of reacting **3** with TMPA.

Reaction of $[Cu_2(Me_2im)_6(O_2)]^{2+}$ (3) with TMPA: Ligand Exchange and Transformation of the Peroxo Complex 3 to $\{Cu(TMPA)\}_2(O_2)]^{2+}$ (4). An important experiment further confirming the formulation and assignment of **3** as a peroxo–dicopper(II) species is the observed reaction of **3** with the TMPA (TMPA = tris[2-(pyridyl)methyl]amine), the ligand present in the X-ray structurally characterized complex $[\{Cu(TMPA)\}_2(O_2)]^{2+}$ (**4**). This transformation can be followed spectrophotometrically, Figure 8. Thus, excess O_2 was removed by application of several vacuum/argon purges from a solution of $[Cu_2(Me_2im)_6(O_2)]^{2+}$ (**3**) in a cuvette assembly, the latter generated by oxygenation of a 2.87 mM solution of **2** at –90 °C.

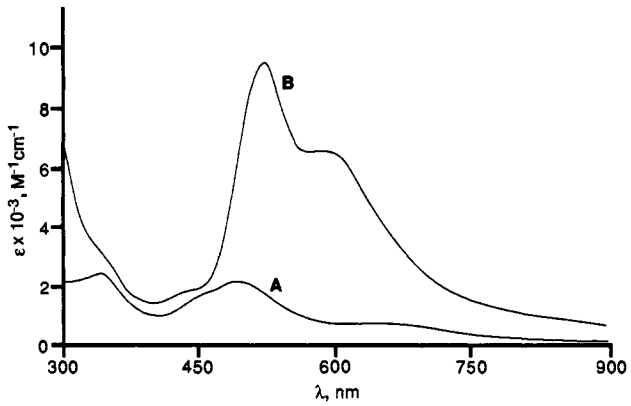

Figure 8. Change in the UV–vis spectrum of $[Cu_2(Me_2im)_6(O_2)]^{2+}$ (**3**) (spectrum A) after addition of TMPA at –90 °C, giving spectrum B which corresponds to $[\{Cu(TMPA)\}_2(O_2)]^{2+}$ (**4**).

The spectrum obtained (A) is that already described. Addition of 2.5 equiv of TMPA (as a CH_2Cl_2 solution under Ar at –90 °C) directly to this solution of **3** caused an immediate change to purple, exhibiting spectrum **B**, Figure 8. From the observed adsorptivity and new volume, calculation of the concentration of $[\{Cu(TMPA)\}_2(O_2)]^{2+}$ (**4**) indicated that there was an 81% conversion of **3** to **4**, based on the known extinction coefficient for the λ_{max} = 525 nm of **4**.[11] This "peroxide transfer" reaction is attributed

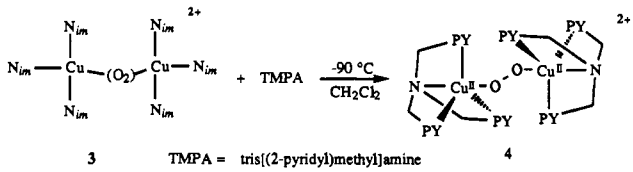

to the lability of the unidentate 1,2-dimethylimidazole ligand and the greater stability of the chelating TMPA ligand complex.

Protonation of $[Cu_2(Me_2im)_6(O_2)]^{2+}$ (3): Generation of H_2O_2. When a solution of the brown dioxygen complex $[Cu_2(Me_2im)_6(O_2)]^{2+}$ (**3**) in CH_2Cl_2 at –90 °C is subjected to protonation by addition of excess (~10 equiv) $HBF_4{\cdot}Et_2O$, an immediate color change to blue occurs with formation of H_2O_2 as determined by an iodometric titration. (Experimental Section). The yield was 74%, based on the amount of **2** used to generated peroxo complex **3**. This result further proves the peroxo nature of **3** and that this

$$[Cu_2(Me_2im)_6(O_2)]^{2+} + 2\,H^+ \rightarrow Cu(II)\ \text{products} + H_2O_2$$
(**3**)

O_2^{2-} ligand is basic, such that protonation and loss of hydrogen peroxide competes favorably with binding to copper(II).

Reaction of $[Cu_2(Me_2im)_6(O_2)]^{2+}$ (3) with Carbon Dioxide: Formation of a Percarbonato Intermediate and Carbonato Product $[Cu_2(Me_2im)_6(CO_3)]^{2+}$ (5). Peroxo–metal complexes are known to react with the electrophilic CO_2 molecule, often forming metal–carbonato products; observation of such behavior is indicative of a metal-coordinated nucleophilic species.[47] Such a reaction is observed for $[Cu_2(Me_2im)_6(O_2)]^{2+}$ (**3**). Introduction of dry CO_2 to a brown solution of **3** causes an immediate change to a blue color with λ_{max} = 350 (ϵ, 1750 M^{-1} cm^{-1}), 615 (ϵ, 240 M^{-1} cm^{-1}) nm, which is stable only at low temperatures (<–60 °C) (Figure 9). When this blue species is allowed to decompose thermally, a green compound is formed with λ_{max} = 360 (ϵ, 1940 M^{-1} cm^{-1}), 712 (ϵ, 350 M^{-1} cm^{-1}) nm (Figure 9). The final green isolated complex is identified as a carbonato–dicopper(II) complex $[Cu_2(Me_2im)_6(CO_3)]^{2+}$ (**5**), based on analytical data, its spectroscopic properties, and its reaction with acid, causing liberation of CO_2. The latter was quantified by passing released gases through a saturated solution of $Ba(OH)_2$ to yield $BaCO_3$ (58%) (Experimental Section).

(45) (a) Zubieta, J.; Karlin, K. D.; Hayes, J. C. In *Copper Coordination Chemistry: Biochemical and Inorganic Perspectives*; Karlin, K. D., Zubieta, J., Eds.; Adenine Press: Albany, NY, 1983; pp 97–108. (b) Karlin, K. D.; Hayes, J. C.; Shi Juen; Hutchinson, J. P.; Zubieta, J. *Inorg. Chem.* **1982**, *21*, 4106–4108. (c) Jacobson, R. R. Ph.D. Dissertation, State University of New York at Albany, 1989. (d) Karlin, K. D.; Dahlstrom, P. L.; Hyde, J. R.; Zubieta, J. *J. Chem. Soc., Chem. Commun.* **1980**, 906–908.

(46) A review on the properties of weakly coordinated anions such as PF_6^- has recently appeared; Strauss, S. H. *Chem. Rev.*, **1993**, *93*, 927–942.

(47) Paul, P. P.; Tyeklár, Z.; Jacobson, R. R.; Karlin, K. D. *J. Am. Chem. Soc.*, **1991**, *113*, 5322–5332 and references cited therein.

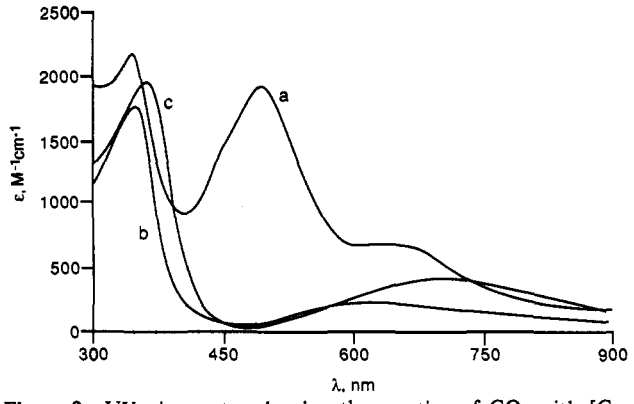

Figure 9. UV–vis spectra showing the reaction of CO_2 with $[Cu_2(Me_2im)_6(O_2)]^{2+}$ (**3**) in CH_2Cl_2 at 90 °C: (a) **3**; (b) blue percarbonato species; (c) $[Cu_2(Me_2im)_6(CO_3)]^{2+}$ (**5**), formed upon warming and then rechilling the solution to –90 °C. See text for further explanation.

Scheme III

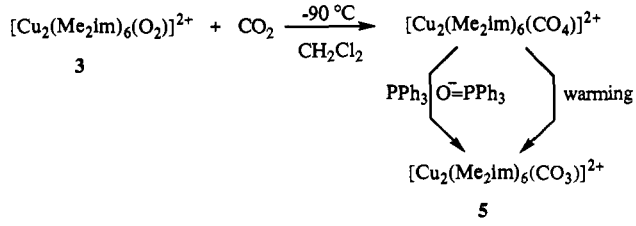

The blue intermediate in the above reaction is presumed to be a peroxo–carbonato (i.e. CO_4^{2-}) species, generated via reaction of CO_2 with the copper(II)-bound peroxide (O_2^{2-}) ligand. A similar intermediate has been observed in the reaction of CO_2 with other Cu_2O_2 complexes such as $[\{Cu(TMPA)\}_2(O_2)]^{2+}$ (**4**) and also in other metal–peroxo compounds.[47] Evidence consistent with the peroxo–carbonato formulation of the blue intermediate and its oxygen atom transfer capability comes from its reaction with PPh_3, which gives $O{=}PPh_3$ and the carbonato–Cu(II) complex $[Cu_2(Me_2im)_6(CO_3)]^{2+}$ (**5**) (Experimental Section). Thus, addition of PPh_3 to the blue solution, followed by slow warming to room temperature gave both **5** and triphenylphosphine oxide (80% converstion), the latter identified and quantified by gas chromatography (Experimental Section). Control reactions indicate that peroxo complex $[Cu_2(Me_2im)_6(O_2)]^{2+}$ (**3**) and $[Cu_2(Me_2im)_6(CO_3)]^{2+}$ (**5**) do not themselves oxygenate PPh_3.

Reaction of $[Cu_2(Me_2im)_6(O_2)]^{2+}$ (3) with CO and PR_3 (R = Ph, Me): Qualitative Determination of O_2 Released and Isolation of $[Cu(Me_2im)_3(PR_3)]^+$ (R = Ph, (**6a**); R = Me (**6b**)). As is the case for O_2 reactivity, carbon monoxide does not react with the linear two-coordinate copper(I) complex $[Cu(Me_2im)_2]^+$ (**1**), again in accord with observations made by Sorrell.[23e] However, the three-coordinate complex $[Cu(Me_2im)_3]^+$ (**2**) does. Binding is not exceptionally strong, but observations of a typical $\nu(CO)$ = 2069 cm^{-1} in CH_2Cl_2 solutions of **2** bubbled with CO, along with *in situ* solution EXAFS measurements,[30] are consistent with the formation of an adduct $[Cu(Me_2im)_3(CO)]^+$. We have previously shown that bubbling CO through –80 °C solutions of various Cu_2O_2 adducts such as $[\{Cu(TMPA)\}_2(O_2)]^{2+}$ (**4**) and $[Cu_2(Nn)(O_2)]^{2+}$ (Scheme II) leads to displacement of the O_2 ligand by CO, with formation of the resulting copper(I)–CO adducts.[11b,13a] We note that no corresponding reaction occurs with $[Cu_2(Me_2im)_6(O_2)]^{2+}$ (**3**), a further indication of the relatively weak CO binding to tricoordinate $[Cu(Me_2im)_3]^+$ (**2**).

As a very good and copper(I) specific ligand, triphenylphosphine has also been previously used by us to displace O_2 from copper–dioxygen adducts such as $[\{Cu(TMPA)\}_2(O_2)]^{2+}$ (**4**),[11] and such reactions do occur in the present 1,2-dimethylimidazole system. Thus, addition of 2 equiv of PPh_3 to a solution of $[Cu_2(Me_2im)_6(O_2)]^{2+}$ (**3**) at –90 °C, followed by slow warming to room temperature, causes displacement of O_2. This was determined by passing the evolved gas through an alkaline pyrogallol test solution, which turns deep brown upon exposure to dioxygen. The phosphine product was $[Cu(Me_2im)_3(PPh_3)](PF_6)$ (**6a**(PF_6)), identified by elemental analysis and NMR spectroscopy. It was obtained in 67% yield, a somewhat low value, thought to arise because of a somewhat inefficient reaction of PPh_3, with **3** decomposing because of the need to warm up the reaction mixture substantially from –90 °C. Using PMe_3 gave better results, presumably because it is more basic and less bulky. Addition of 2 equiv caused bleaching of the typical color of solutions of **3** even at –90 °C, and O_2 was again evolved according to the pyrogallol test. The copper(I)–phosphine adduct $[Cu(Me_2im)_3(PMe_3)]^+$ (**6b**) was isolated in >80% yield.

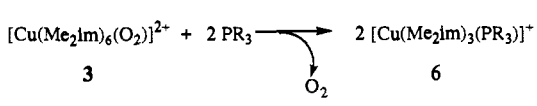

Summary/Conclusions

The copper-1,2-dimethylimidazole system described in this paper provides insight into some of the factors which control dioxygen binding and reactivity in imidazole-ligated copper complexes, and perhaps proteins. As previously documented by Sorrell, linear two-coordinate Cu(I)–imidazole complexes are unreactive to O_2 and CO.[23e] On the other hand, the coordination of a third (imidazole) ligand imparts reactivity toward both dioxygen and carbon monoxide. The three-coordinate precursor complex $[Cu(Me_2im)_3]^+$ (**2**) is best described as a highly distorted, probably T-shaped structure, and when reacted with O_2 at –90 °C, it gives a dioxygen adduct formulated as the peroxodicopper(II) complex $[Cu_2(Me_2im)_6(O_2)]^{2+}$ (**3**), based on its physical properties and reactivity.

Insights into the solution structure of **3** have been obtained via X-ray absorption spectroscopy, and these reveal two possible structures, an end-on bridged compound (i.e., *trans* μ-1,2-peroxo) **A**, or an unusual very bent side-on μ-η^2:η^2-peroxo structure with short Cu···Cu distance of ~2.8 Å, **B**. While in some respects the latter structure better fits the XAS data, the limitations and constraints of the technique make it difficult to absolutely distinguish between the two possibilities.

However, on the basis of chemistry and spectroscopy, we prefer the end-on bound structure **A** as the more likely structure of $[Cu_2(Me_2im)_6(O_2)]^{2+}$ (**3**). The reactivity of **3** much more resembles that of $[\{Cu(TMPA)\}_2(O_2)]^{2+}$ (**4**) with *trans* μ-1,2-peroxo–dicopper(II) moiety which is basic or nucleophilic in its reactions with substrates such as H^+, carbon dioxide and tertiary phosphines; the reactions of these reagents with the side-on bound peroxo–copper complexes $[Cu_2(N_n)(O_2)]^{2+}$ (n = 4, Scheme II) is quite different. However, such a conclusion must be tempered by other observations recently made by Sorrell[48] or those made by Kitajima on $[(HB(3,4\text{-}iPr_2pz)_3)Cu]_2(O_2)$,[14,49] since they find instances where it is clear that not all Cu_2O_2 complexes will fall clearly into one such reactivity category or the other. Considerable additional studies in reactivity/structure correlations will need to be made. Another factor which would seem to favor structure **A** for $[Cu_2(Me_2im)_6(O_2)]^{2+}$ (**3**) is the absence of an intense ($\epsilon \sim$ 20 000) near-UV band in the ~350-nm region, a spectroscopic signature for the planar μ-η^2:η^2-peroxo structure in oxyhemocyanin, in Kitajima's model complex $[(HB(3,4\text{-}iPr_2pz)_3)Cu]_2(O_2)$,[50] and in the putative bent side-on peroxo groups in $[Cu_2(N_n)(O_2)]^{2+}$ (Scheme II).[13a] However, the severely bent structure **B** could conceivably diminish the expected intensity for this peroxo-π^*_σ

(48) Sorrell, T. N.; Garrity, M. L.; Richards, J. L.; Pigge, F. C.; Allen, W. E. In ref 1b, pp 338–347.
(49) Katajima, N.; Koda, T.; Iwata, Y.; Moro-oka, Y. *J. Am. Chem. Soc.* **1990**, *112*, 8833–8839.
(50) Baldwin, M. J.; Root, D. E.; Pate, J. E.; Fujisawa, K.; Kitajima, N.; Solomon, E. I. *J. Am. Chem. Soc.* **1992**, *114*, 10421–10431.

→ Cu(II) transition. Additional spectral differences between **3** and **4** might be due to geometric and ligation changes, i.e. a tetragonal N_3O ligand donor set for **3** (*d–d* band at 650 nm, *vide supra*), but coordination of N_4O trigonal bipyriamidal copper(II) in **4**. Whether on the basis of reactivity comparisons or spectroscopy, any conclusions cannot be firm, since there are as yet only two very well characterized Cu_2O_2 complexes with known structure, assigned spectroscopy and well-established reactivity.[11,14] Undoubtedly, such properties will be fine-tuned by perturbations in ligand structure, its particular donating capacities and steric or coordination constraints imparted to resulting copper complexes. Clearly, more Cu_2O_2 complexes need to be described.

The relevance of compounds **1–3** lies in the fact that their reaction chemistry with CO and O_2 mimics aspects of copper proteins such as hemocyanin, tyrosinase, dopamine β hydroxylase, and possibly other enzymes. Distinctive features include the modeling of the reactivity of the putative enzymatic Cu(I) sites with respect to (i) imidazole ligation, (ii) two- or three-coordination of the precursor complex, and (iii) dioxygen and carbon monoxide binding. The structural data presented here, together with a large literature on the structure of Cu(I) complexes of other ligand systems which act as model monooxygenase precursors,[33,34] seem to suggest that distorted trigonal (pseudo-T-shaped) Cu(I) stereochemistry may be a prerequisite for O_2 binding and/or monooxygenase activity. The possibility of μ-η^2:η^2-coordination in $[Cu_2(Me_2im)_6(O_2)]^{2+}$ (**3**) further emphasizes the importance of side-on dioxygen binding to copper ion,[13b,14,34,50] and we suggest this mode of coordination could be of significance not only in dinuclear copper systems but also in complexes or proteins with mononuclear sites. Further experiments and new ligand design to test these ideas are underway.

Acknowledgment. This work was supported by Grant R01 GM28962 (K.D.K.) and Grant R01 NS-27583 (N.J.B.) from the National Institutes of Health and Grant RR01 633-10 to the National Biostructures PRT at the NSLS, Brookhaven National Lab. We thank Professor S. J. Lippard for the gift of the [Cu_2(μ-DMAD)(TC-6,6)] complex.

Supplementary Material Available: Tables with details of the X-ray structural study of **1** (experimental procedures, positional and thermal parameters, and complete bond lengths and angles) and full parameter sets for the simulations of the EXAFS data, as generated by the program EXCURV (20 pages). Ordering information is given on any current masthead page.